

Tackling Complex Conditions in Unsupervised Combinatorial Optimization: Cardinality, Minimum, Covering, and More

Anonymous Authors¹

Abstract

Combinatorial optimization (CO) is naturally discrete, making machine learning based on differentiable optimization inapplicable. Karalias & Loukas (2020) adapted the probabilistic method to incorporate CO into differentiable optimization. Their work ignited the research on unsupervised learning for CO, composed of two main components: probabilistic objectives and derandomization. However, each component confronts unique challenges. First, deriving objectives under complex conditions is nontrivial. Second, the derandomization process is underexplored, and the existing derandomization methods are either random sampling or naive rounding. In this work, we aim to tackle complex conditions in unsupervised CO. First, we concretize the targets for objective construction and derandomization with theoretical justification. Then, for various complex conditions commonly involved in different CO problems, we derive nontrivial objectives and derandomization to meet the targets. Finally, we apply the derivations to various CO problems. Via extensive experiments on synthetic and real-world graphs, we validate the correctness of our derivations and show our empirical superiority w.r.t. both optimization quality and speed.

1. Introduction

Combinatorial optimization (CO) problems are *discrete* by their nature. Machine learning methods are based on differentiable optimization (e.g., gradient descent), and applying them to CO is non-trivial. In their pioneering work, Karalias & Loukas (2020) adapted the probabilistic method (Erdős & Spencer, 1974; Alon & Spencer, 2016) to incorporate discrete CO problems into differentiable optimization. Specifically, they proposed to evaluate CO objectives on a *distribution*

of discrete choices (i.e., in a *probabilistic* manner), allowing for the differentiable optimization-based ML techniques to be applied to CO problems. This ignited the line of research on unsupervised (i.e., not supervised by solutions) learning for combinatorial optimization (UL4CO).

In UL4CO, we have two components: (1) construction of *probabilistic objectives* and (2) *derandomization* to obtain the final discrete solutions. However, the prior works on UL4CO share multiple limitations. First, although some desirable properties of probabilistic objectives (e.g., *desirable objectives should be differentiable, and they should align well with the original discrete objectives*) have been proposed, how to derive objectives satisfying such properties is still unclear, especially under complex conditions.¹ At the same time, the derandomization process is underexplored, without many practical techniques or theoretical discussions. Specifically, the existing derandomization methods are either random sampling or naive rounding. *Random sampling, by its nature, may cost us a large number of samplings and good luck to have good results; while the performance of naive rounding may highly depend on the order of rounding and end up with mediocre solutions. They only guarantee, at best, derandomized solutions are no worse than the given continuous solutions. However, how to obtain stronger guarantees in an efficient way has been an open problem.*

Motivated by the limitations, we study and propose UCOM2 (Unsupervised **C**ombinatorial Optimization Under **C**omplex Conditions). Specifically, our contributions are four-fold.

- **We concretize the targets for objective construction and derandomization with theoretical justification (Sec. 3).** We theoretically show that probabilistic objectives that can be rephrased as an expectation are desirable, and propose a fast and effective derandomization scheme with a quality guarantee stronger than the existing ones.
- **We derive non-trivial objectives and derandomization for various complex conditions to meet the targets (Sec. 4).** We focus on conditions that are mathematically hard to handle but commonly involved in CO problems, e.g., cardinality constraints, minimum, and covering.

¹In this work, we focus on objectives and constraints that have not been systematically handled within the UL4CO framework (and thus we believe they are nontrivial to tackle) and are commonly involved in various CO problems.

¹Anonymous Institution, Anonymous City, Anonymous Region, Anonymous Country. Correspondence to: Anonymous Author <anon.email@domain.com>.

Preliminary work. Under review by the International Conference on Machine Learning (ICML). Do not distribute.

- **We apply our derivations to different CO problems involving such complex conditions (Sec. 5).** For each problem, we analyze what conditions are involved and derive objectives and derandomization by combining our derivations for the involved conditions.
- **We show the empirical superiority of UCOM2 via experiments (Sec. 6).** Equipped with our derivations, our method UCOM2 achieves better optimization quality and speed across different CO problems on both synthetic and real-world graphs, outperforming various baselines.

Reproducibility. The code and datasets are available in the online appendix (Anonymous, 2024).

2. Preliminaries and Background

2.1. Preliminaries

Graphs. A graph $G = (V, E, W)$ is defined by a *node set* V , an *edge set* E , and *edge weights* $W : E \rightarrow \mathbb{R}$. We let $n = |V|$ denote the number of nodes (WLOG, $V = [n] := \{1, 2, \dots, n\}$), and let $m = |E|$ denote the number of edges.

Combinatorial optimization. We consider *combinatorial optimization* (CO) problems on graphs with discrete *decisions* on nodes. Each CO problem can be represented by a tuple (f, \mathcal{C}, d) with (1) an *optimization objective* $f : d^n \rightarrow \mathbb{R}_+$, (2) *constraints* defined by a *feasible set* $\mathcal{C} \subseteq d^n$, and (3) a set of *possible decisions* d (on each $v \in V$). Given decisions $X_v \in d$ with $v \in V$, we have a *full decision* $X \in d^n$.

For each graph $G = (V, E, W)$, we can use the optimization objective function f to evaluate each full decision $X \in d^n$ on G by $f(X; G)$, and we aim to *solve* $\min_{X \in \mathcal{C}(G)} f(X; G)$. By default, we consider CO problems with *binary* decisions (i.e., $d = \{0, 1\}$).² Given $X \in \{0, 1\}^n$, we call each node v with $X_v = 1$ a *chosen node*, and call $V_X := \{v \in V : X_v = 1\} \subseteq V$ the *chosen subset* (i.e., the set of chosen nodes).

2.2. Background: UL4CO

We shall introduce the background of unsupervised learning for combinatorial optimization (UL4CO), including the overall pipeline and some existing ideas/techniques.³

2.2.1. THE UL4CO PIPELINE: ERDŐS GOES NEURAL

The UL4CO pipeline, Erdős Goes Neural (Karalias & Loukas, 2020), is based on the probabilistic method (Erdős & Spencer, 1974), with three components: objective construction, differentiable optimization, and derandomization.

Probabilistic objective construction. The high-level idea is to evaluate discrete objectives on a distribution of decisions, which accepts continuous parameterization. Specifically, given a CO problem $(f : \{0, 1\}^n \rightarrow \mathbb{R}, \mathcal{C}, d = \{0, 1\})$,⁴ we first construct a *penalized* objective $f_{\text{pen}}(X) = f(X) + \beta \mathbf{1}(X \notin \mathcal{C})$ with *constraint coefficient* $\beta > 0$. Then, a *prob-*

abilistic objective $\tilde{f} : [0, 1]^n \rightarrow \mathbb{R}$ accepting probabilistic (and thus continuous) inputs is constructed such that

$$\tilde{f}(p) \geq \mathbb{E}_{X \sim p} f_{\text{pen}}(X) = \mathbb{E}_{X \sim p} f(X) + \beta \Pr_{X \sim p}[X \notin \mathcal{C}].$$

We see each $p \in [0, 1]^n$ as a vector of probabilities, with p_v 's being *independent Bernoulli* variables.⁵ Hence, we have

$$\Pr_p[X] = \prod_{v \in V_X} p_v \prod_{u \in V \setminus V_X} (1 - p_u),$$

$$\mathbb{E}_{X \sim p} f(X) = \sum_{X \in \{0, 1\}^n} \Pr_p[X] f(X), \text{ and}$$

$$\Pr_{X \sim p}[X \notin \mathcal{C}] = \sum_{X \in \{0, 1\}^n \setminus \mathcal{C}} \Pr_p[X] = 1 - \sum_{X \in \mathcal{C}} \Pr_p[X].$$

Differentiable optimization. For *differentiable* optimization, we need to ensure that \tilde{f} is differentiable (w.r.t. p). At this moment, let us assume we have constructed such a \tilde{f} . Then, given a graph G , we can use differentiable optimization (e.g., gradient descent) to obtain optimized probabilities p_o with (ideally) small $\tilde{f}(p_o; G)$.

Derandomization. Finally, *derandomization* is used to obtain deterministic full decisions. For each test instance G , the derandomization process transforms each $p_o \in [0, 1]^n$ obtained by probabilistic optimization into a *discrete* (i.e., deterministic) full decision $X_p \in \{0, 1\}^n$. Karalias & Loukas (2020) showed a quality guarantee of derandomization by *random sampling*. See App. B for more details.

2.2.2. LOCAL DERANDOMIZATION

The theoretical quality guarantee by Karalias & Loukas (2020) is obtained by random sampling, and we may need a large number of samplings (and good luck) to have a good bound. Wang et al. (2022) further *proved a deterministic* (i.e., *not relying on random sampling*) *quality guarantee by iterative rounding* (i.e., a series of local derandomization along with a node enumeration). Notably, Karalias & Loukas (2020) essentially proposed and used *iterative rounding* but Wang et al. (2022) *first formalized it with theoretical guarantee*. The principle of iterative rounding involves two concepts: (1) *local derandomization* of probabilities p and (2) *entry-wise concavity* of probabilistic objective \tilde{f} .

Local derandomization. Given $p \in [0, 1]^n$, $i \in [n]$, and $x \in \{0, 1\}$, $\text{der}(i, x; p) \in [0, 1]^n$ is the result after p_i being *locally derandomized* as x , i.e.,
$$\begin{cases} \text{der}(i, x; p)_i = x, \\ \text{der}(i, x; p)_j = p_j, \forall j \neq i. \end{cases}$$

Entry-wise concavity. A probabilistic objective $\tilde{f} : [0, 1]^n \rightarrow \mathbb{R}$ is *entry-wise concave* if $\forall p \in [0, 1]^n$ and $i \in [n]$,

$$p_i \tilde{f}(\text{der}(i, 1; p)) + (1 - p_i) \tilde{f}(\text{der}(i, 0; p)) \leq \tilde{f}(p).$$

Wang et al. (2022) showed that applying a series of local derandomization with an entry-wise concave objective \tilde{f} does not increase the objective. See App. B for more details.

⁵ Assuming independent Bernoulli variables gives simplicity and tractability, while other ways to model decision distributions, e.g., other distributions (Karalias et al., 2022) and considering dependency between variables (Sanokowski et al., 2023), are potential directions for future exploration.

²We will discuss non-binary cases in Sec. 4.5.

³See App. C for more extensive related work.

⁴Karalias & Loukas (2020) only considered binary problems.

3. Concretizing Targets: What Do We Need?

First, we aim to concretize the targets for objective construction and derandomization to guide our further derivations.

3.1. Good objectives: Expectations are all you need

Good properties. We summarize some known *good* properties of a probabilistic objective \tilde{f} (Karalias & Loukas, 2020; Wang et al., 2022): (P1) $\tilde{f} : [0, 1]^n \rightarrow \mathbb{R}$ accepts *continuous* inputs $p \in [0, 1]^n$ (rather than discrete $X \in \{0, 1\}^n$), (P2) \tilde{f} is an *upper bound* of the expectation of a penalized objective $f + \beta \mathbb{1}(X \notin \mathcal{C})$ for some $\beta > 0$, (P3) \tilde{f} is *differentiable* w.r.t. p , and (P4) \tilde{f} is *entry-wise concave* w.r.t. p . We include an additional desirable property that has been discussed (Karalias & Loukas, 2020; Karalias et al., 2022; Kolloviev et al., 2024) but has not been explicitly formalized for UL4CO: (P5) $\min_p \tilde{f}(p) = \min_X f(X)$ and $\arg \min_p \tilde{f}(p) = \arg \min_X f(X)$, i.e., when we minimize \tilde{f} , we also minimize the original objective f . It also avoids meaningless \tilde{f} , e.g., a constant function with a very high value (which satisfies (P1)-(P4) but not (P5)).

High-level Target 1 (Good objectives). Given an optimization objective $f : \{0, 1\}^n \rightarrow \mathbb{R}$ and constraints $X \in \mathcal{C}$, we aim to construct a good probabilistic objective $\tilde{f} : [0, 1]^n \rightarrow \mathbb{R}$ to satisfy all the good properties (P1)-(P5).

Below, we show that a specific form of objectives satisfies all the good properties. First, *expectations are all you need*, i.e., any probabilistic objective that is the expectation of any discrete function satisfies properties (P1), (P3), and (P4).

Theorem 1 (Expectations are all you need). *For any $g : \{0, 1\}^n \rightarrow \mathbb{R}$, $\tilde{g} : [0, 1]^n \rightarrow \mathbb{R}$ with $\tilde{g}(p) = \mathbb{E}_{X \sim p} g(X)$ is differentiable and entry-wise concave w.r.t. p .*

Proof. See App. A for all the proofs. \square

Remark 1. Differentiability and entry-wise concavity are closed under addition. Hence, a linear combination of expectations is also differentiable and entry-wise concave. Also, probabilities are special expectations of indicator functions. The differentiability of expectation may not hold when p_v 's are not independent Bernoulli variables, e.g., when the expectation is taken with Lovasz extension (Bach et al., 2013).

To further satisfy (P2) and (P5), we only need to find a tight upper bound (TUB) of a penalized objective.

Definition 1 (Tight upper bounds). Given $g : \{0, 1\}^n \rightarrow \mathbb{R}$, we say $\hat{g} : \{0, 1\}^n \rightarrow \mathbb{R}$ is a *tight upper bound* (TUB) of g , iff (i.e., if and only if) $\hat{g}(X) \geq g(X)$, $\forall X$ with $\min_X \hat{g}(X) = \min_X g(X)$ and $\arg \min_X \hat{g}(X) = \arg \min_X g(X)$, where $\arg \min_X g(X) = \{X^* : g(X^*) = \min_X g(X)\}$.

Remark 2. It is easy to see that $\hat{g} = g$ is always a TUB of g . When $g = \mathbb{1}[X \notin \mathcal{C}]$ is an indicator function for the violation of constraints $X \in \mathcal{C}$, the condition in Def. 1 is equivalent to $\hat{g}(X) \geq 1$, $\forall X \notin \mathcal{C}$ and $\hat{g}(X) = 0$, $\forall X \in \mathcal{C}$.

To conclude, we propose the following concretized target to construct *the expectation of a tight upper bound*.

Target 1 (Construct the expectation of a TUB). *Given $f : \{0, 1\}^n \rightarrow \mathbb{R}$ with constraints $X \in \mathcal{C}$, let $g(X) = \mathbb{1}(X \notin \mathcal{C})$, we aim to find $\hat{f}_1, \hat{f}_2 : \{0, 1\}^n \rightarrow \mathbb{R}$ such that \hat{f}_1 is a TUB of f and \hat{f}_2 is a TUB of g , and to construct a probabilistic objective $\tilde{f}(p) := \mathbb{E}_{X \sim p} \hat{f}_1(X) + \beta \mathbb{E}_{X \sim p} \hat{f}_2(X)$ with $\beta > 0$.*

3.2. Fast and effective derandomization: Do it in a greedy and incremental manner

High-level Target 2 (Fast and effective derandomization). We aim to propose a derandomization scheme that is *fast* in speed and *effective* in generating high-quality solutions.

Greedy. To this end, we generalize *greedy* algorithms to greedy derandomization and propose an *incremental* scheme to improve the speed. For greedy derandomization, starting from $p_{\text{cur}} = p_o$, we repeat the following steps:

- (1) greedily finding the best local derandomization, i.e., $(i^*, x^*) \leftarrow \arg \min_{(i, x) \in [n] \times \{0, 1\}} \tilde{f}(\text{der}(i, x; p_{\text{cur}}))$;
- (2) conducting the best derandomization, i.e., $p_{\text{cur}} \leftarrow \text{der}(i^*, x^*; p_{\text{cur}})$.

Theorem 2 (Goodness of greedy derandomization). *For any entry-wise concave f and any $p_o \in [0, 1]^n$, the above process of greedy derandomization can always reach a point where the final p_{final} is (G1) discrete (i.e., $p_{\text{final}} \in \{0, 1\}^n$), (G2) no worse than p_o (i.e., $\tilde{f}(p_{\text{final}}) \leq \tilde{f}(p_o)$), and (G3) a local minimum (i.e., $\tilde{f}(p_{\text{final}}) \leq \min_{(i, x) \in [n] \times \{0, 1\}} \tilde{f}(\text{der}(i, x; p_{\text{final}}))$).*

Remark 3. Our two theorems are synergic. Specifically, Thm. 1 guarantees an entry-wise concave probabilistic objective \tilde{f} , which is used as a condition in Thm. 2.

Greedy derandomization improves upon the existing derandomization methods. Specifically, random sampling (Karalias & Loukas, 2020) guarantees (G1), and iterative rounding (Wang et al., 2022) guarantees (G1) and (G2). However, challenges arise regarding the time complexity since a naive way requires $2n$ evaluations of \tilde{f} at each step.

Incremental. To this end, we propose to conduct the derandomization in an *incremental* manner to increase the speed, which gives the following target.

Target 2 (Conduct incremental greedy derandomization). *We conduct greedy derandomization and improve the speed by deriving the incremental differences (IDs) $\Delta \tilde{f}(i, x, p_{\text{cur}}) := \tilde{f}(\text{der}(i, x; p_{\text{cur}})) - \tilde{f}(p_{\text{cur}})$ for all the (i, x) pairs, instead of evaluating the “whole” function, i.e., $\tilde{f}(\text{der}(i, x; p_{\text{cur}}))$'s.⁶*

4. Deriving Formulae to Meet the Targets

The targets in Sec. 3 provide us guidelines, while deriving objectives and derandomization to meet those targets is

⁶Usually, the incremental differences are simpler than the whole function, and are easily parallelizable.

nontrivial. In this work, we focus on UCOM2 (Unsupervised Combinatorial Optimization Under Complex Conditions) and baptize our method with the same name. For various complex conditions that are commonly involved in different CO problems (see Sec. 5 and App. F), we shall derive (1) TUB-based probabilistic objectives \hat{f} to meet Target 1 and (2) incremental differences (IDs) of \hat{f} to meet Target 2. Some complex conditions were encountered in the existing works but were not properly handled within the probabilistic UL4CO pipeline. See more discussions in App. B.3. We tackle each condition using the template below. However, this does not imply that it is trivial. Deriving TUB and IDs for each condition requires distinct, non-trivial ideas.

Construct a probabilistic objective to meet Target 1:

- (S1-1) We find a TUB \hat{f} for the condition i.e. Given an optimization objective f , we find \hat{f} s.t. $\hat{f}(X) \geq f(X), \forall X$ with $\min_X \hat{f}(X) = \min_X f(X)$ and $\arg \min_X \hat{f}(X) = \arg \min_X f(X)$
 - OR Given a constraint $X \in \mathcal{C}$, we find \hat{f} s.t. $\hat{f}(X) \geq \mathbb{1}(X \notin \mathcal{C}), \forall X$ with $\hat{f}(X) = 0, \forall X \in \mathcal{C}$
 - (S1-2) After finding \hat{f} , we derive $\hat{f}(p) := \mathbb{E}_{X \sim p} \hat{f}(X)$
- Derive derandomization to meet Target 2:**
- (S2) We derive the formula of IDs $\Delta \hat{f}(\text{der}(i, x; p))$

The conditions to be tackled below have both theoretical and empirical values. Specifically, they are mathematically hard to handle for probabilistic UL4CO, and are commonly involved in many CO problems.

4.1. Cardinality constraints

Definition. We consider constraints $X \in \mathcal{C}$ with $\mathcal{C} = \{X : |V_X| \in C_c\}$. Some typical cases are $C_c = \{k\}$ or $C_c = \{t \in \mathbb{N} : t \leq k\}$ for some $k \in \mathbb{N}$ (Buchbinder et al., 2014).⁷ Given $p \in [0, 1]^n$, $|V_X| = \sum_{i \in V} X_i$ (see Sec. 2) follows a Poisson binomial distribution $\text{PoiBin}(p_1, p_2, \dots, p_n)$ with parameters $(p_i)_{i \in [n]}$ (Wang, 1993). The probability mass function (PMF) is for each $0 \leq t \leq n$,

$$\Pr_{X \sim p}[|V_X| = t] = \sum_{V_t \subseteq V : |V_t| = t} \prod_{i \in V_t} p_i \prod_{j \in V \setminus V_t} (1 - p_j).$$

(S1-1). We find $\hat{f}_{\text{card}}(X; C_c) := \min_{k \in C_c} ||V_X| - k|$,⁸ i.e., the minimum distance to the feasible cardinality set C_c .

Lemma 1. \hat{f}_{card} is a TUB of $\mathbb{1}[X \notin \mathcal{C}]$.

(S1-2). We derive $\tilde{f}_{\text{card}}(p; C_c) := \mathbb{E}_{X \sim p} \hat{f}_{\text{card}}(X; C_c) = \sum_{t \in [n] \setminus C_c} \Pr_{X \sim p}[|V_X| = t] \min_{k \in C_c} |t - k|$. The main

⁷Enforcing cardinality constraints at test time (e.g., taking top- k) is easy but differentiable training with cardinality constraints is nontrivial. Other than probabilistic-method UL4CO, Sinkhorn-related techniques (Sinkhorn & Knopp, 1967; Wang et al., 2023) are valid ways. See also our discussions in App. B.3.

⁸We can directly compute $\Pr_{X \sim p}[|V_X| \notin C_c]$, but the formula we use practically performs better, intuitively because it distinguishes different levels of violations and works more smoothly. See similar ideas by Pogancic et al. (2019).

technical difficulty is computing the PMF of a Poisson binomial distribution, for which we adopt a discrete-Fourier-transform-based method. The main formula of $\Pr_{X \sim p}[|V_X| = t]$ (See Eq. (6) by Hong (2013)) is

$$\frac{1}{n+1} \sum_{s=0}^n \exp(-i\omega s t) \prod_{j=1}^n (1 - p_j + p_j \exp(i\omega s)),$$

where $i = \sqrt{-1}$ and $\omega = \frac{2\pi}{n+1}$. See App. D.1 for more details.

(S2). We derive the IDs of \hat{f}_{card} , using the recursive formula of the Poisson binomial distribution.

Lemma 2 (IDs of \hat{f}_{card}). For any $p \in [0, 1]^n$, $i \in [n]$, and $0 \leq t \leq n$, let $q_s := \Pr_{X \sim p}[|V_X| = s]$ and $q'_s := \Pr_{X \sim p}[|V_X \setminus \{i\}| = s]$, $\forall s$, we have

$$q'_t = (1 - p_i)^{-1} \sum_{s=0}^t q_s \left(\frac{p_i}{p_i - 1} \right)^{t-s} \quad (\text{if } p_i \neq 1) \quad (1)$$

$$= (p_i)^{-1} \sum_{s=0}^{n-t-1} q_{t+s+1} \left(\frac{p_i - 1}{p_i} \right)^s \quad (\text{if } p_i \neq 0). \quad (2)$$

Based on that, we have

$$\begin{cases} \Delta \tilde{f}_{\text{card}}(i, 0, p; C_c) = \sum_{t \in [n] \setminus C_c} (q'_t - q_t) \min_{k \in C_c} |t - k|, \\ \Delta \tilde{f}_{\text{card}}(i, 1, p; C_c) = \sum_{t \in [n] \setminus C_c} (q'_{t-1} - q_t) \min_{k \in C_c} |t - k|. \end{cases}$$

Remark 4. In practice, we always make sure each $p_i \in [\epsilon, 1 - \epsilon]$ for some small $\epsilon > 0$ for better numerical stability. We use Eq. (1) for $p_i \leq 0.5$ and Eq. (2) for $p_i > 0.5$.

4.2. Minimum (or maximum) w.r.t. a subset

Definition. We consider constraints where we have a pairwise score function (e.g., distance) $h : V \times V \rightarrow \mathbb{R}$ and we aim to compute $f_{\text{ms}}(X) := \min_{v_X \in V_X} h(i, v_X)$ for some $i \in V$ (e.g., the shortest distance to a set of points).

We fix $i \in V$ in the analysis below, and let v_1, v_2, \dots, v_n be a permutation of $V = [n]$ such that $d_1 \leq d_2 \leq \dots \leq d_n$, where $d_j = h(i, v_j), \forall j \in [n]$.

(S1-1). We find $\hat{f}_{\text{ms}}(X; i, h) := \min_{v_X \in V_X} h(i, v_X)$, which is the original objective f_{ms} .

Lemma 3. \hat{f}_{ms} is a TUB of f_{ms} .

(S1-2). We derive $\tilde{f}_{\text{ms}}(p; i, h) := \mathbb{E}_{X \sim p} \hat{f}_{\text{ms}}(X; i, h)$, by decomposing the objective into sub-terms.

Lemma 4. For any $p \in [0, 1]^n$, $\mathbb{E}_{X \sim p} \hat{f}_{\text{ms}}(X; i, h) = p_{v_1} d_1 + (1 - p_{v_1}) p_{v_2} d_2 + \dots + (\prod_{j=1}^{n-1} (1 - p_{v_j})) p_{v_n} d_n$.

(S2). We derive the IDs of \tilde{f}_{ms} , by analyzing which sub-terms are changed after one step of local derandomization.

Lemma 5 (IDs of \tilde{f}_{ms}). For any $p \in [0, 1]^n$ and $j \in [n]$, let $q_j := (\prod_{k=1}^{j-1} (1 - p_{v_k})) p_{v_j}$, the coefficient of d_j in \tilde{f}_{ms} . Then
$$\begin{cases} \Delta \tilde{f}_{\text{ms}}(v_j, 0, p; i, h) = -q_j d_j + \frac{p_{v_j}}{1 - p_{v_j}} \sum_{j' > j} q_{j'} d_{j'}, \\ \Delta \tilde{f}_{\text{ms}}(v_j, 1, p; i, h) = \sum_{j' > j} q_{j'} (d_j - d_{j'}). \end{cases}$$

Remark 5. When $p_{v_j} = 1$, we replace $\frac{p_{v_j}}{1 - p_{v_j}} \sum_{j' > j} q_{j'} d_{j'}$ by $\sum_{j' > j} (\prod_{1 \leq i' \leq i-1, i' \neq j} (1 - p_{v_{i'}})) p_{v_{i'}} d_{j'}$. Since we make sure each $p_i \neq 1$ (see Rem. 4), this does not happen in practice.

4.3. Covering

Definition. We consider conditions where some $i \in V$ needs to be *covered* (i.e., at least one neighbor of i is chosen). Formally, the constraints are $X \in \mathcal{C}$ with $\mathcal{C} = \{X: \{v_X \in V_X: (v_X, i) \in E\} \neq \emptyset\}$.

(S1-1). We find $\hat{f}_{cv}(X; i) := \mathbb{1}(X \notin \mathcal{C})$, which is the *indicative function of the original constraint*.

Lemma 6. \hat{f}_{cv} is a TUB of $\mathbb{1}(X \notin \mathcal{C})$.

(S1-2). We drive $\tilde{f}_{cv}(p; i) := \mathbb{E}_{X \sim p} \hat{f}_{cv}(X; i) = \Pr_{X \sim p}[\{v_X \in V_X: (v_X, i) \in E\} \neq \emptyset]$, by *decomposing the objective into sub-terms*.

Lemma 7. For any $p \in [0, 1]^n$ and $i \in [n]$, $\Pr_{X \sim p}[\{v_X \in V_X: (v_X, i) \in E\} \neq \emptyset] = \prod_{v \in [n]: (v, i) \in E} (1 - p_v)$.

(S2). We derive the IDs of \tilde{f}_{cv} , by *analyzing which sub-terms are changed after one step of local derandomization*.

Lemma 8 (IDs of \tilde{f}_{cv}). For any $p \in [0, 1]^n$ and $i \in [n]$, if $(i, j) \notin E$, then $\Delta \tilde{f}_{cv}(j, 0, p; i) = \Delta \tilde{f}_{cv}(j, 1, p; i) = 0$; if $(i, j) \in E$, then $\begin{cases} \Delta \tilde{f}_{cv}(j, 0, p; i) = p_j \prod_{v \in N_i, v \neq j} (p_v - 1), \\ \Delta \tilde{f}_{cv}(j, 1, p; i) = -\tilde{f}_{cv}(p; i). \end{cases}$

4.4. Cliques (or independent sets)

Definition. We consider conditions where the chosen nodes V_X should form a clique.⁹ Formally, the constraints are $X \in \mathcal{C}$ with $\mathcal{C} = \{X: \binom{V_X}{2} \subseteq E\}$.

(S1-1). We find $\hat{f}_{cq}(X) := |\{(u, v) \in \binom{V_X}{2}: (u, v) \notin E\}|$, the *number of chosen node pairs violating the constraints*.

Lemma 9. \hat{f}_{cq} is a TUB of $\mathbb{1}[X \notin \mathcal{C}]$.

(S1-2). We derive $\tilde{f}_{cq}(p) := \mathbb{E}_{X \sim p} \hat{f}_{cq}(X)$, by *decomposing the objective into sub-terms*.

Lemma 10. For any $p \in [0, 1]^n$, $\mathbb{E}_{X \sim p} \hat{f}_{cq}(X) = \sum_{(u, v) \in \binom{V}{2} \setminus E} p_u p_v$.

(S2). We derive the IDs of \tilde{f}_{cq} , by *analyzing which sub-terms are changed after one step of local derandomization*.

Lemma 11 (IDs of \tilde{f}_{cq}). For any $p \in [0, 1]^n$ and $i \in [n]$,

$$\begin{cases} \Delta \tilde{f}_{cq}(i, 0, p) = -p_i \sum_{j \in [n], j \neq i, (i, j) \notin E} p_j, \\ \Delta \tilde{f}_{cq}(i, 1, p) = (1 - p_i) \sum_{j \in [n], j \neq i, (i, j) \notin E} p_j. \end{cases}$$

Notes. Karalias & Loukas (2020) essentially considered the “cliques” conditions and derived the same formula of $\tilde{f}_{cq}(p)$. But our derivation of the IDs is novel, and we will also show how we can extend this to non-binary cases, which were not discussed. Moreover, our targets and templates provide insights into obtaining and interpreting the derivation.

4.5. Non-Binary Decisions

Definition. We have been considering problems with binary decisions. We also consider *non-binary decisions*, i.e., there

⁹Equivalently, an independent set in the complement graph.

are (potentially) more than two decisions ($|d| \geq 2$). WLOG, we assume that $d = \{0, 1, \dots, c-1\}$ for some $c \geq 2$. Typical examples include problems with partition or coloring.

Our theoretical analysis can be extended to non-binary cases. See App. E.1 for more details.

4.6. Uncertainty

We also consider *uncertainty* in edge existence, i.e., edge probabilities $P: E \rightarrow [0, 1]$. Due to the generality of non-binary conditions and uncertainty, the details of objective construction and derandomization will be deferred to where each specific problem is analyzed in Sec. 5.

Notes. Throughout the section, two commonly used ideas for constructing TUBs are: (1) using a function itself (Lems. 3 & 6), and (2) relaxing the binary “a constraint is violated” to “the number of violations” (Lems. 1 & 9). Moreover, techniques commonly used in our derivations include (1) decomposing objectives into sub-terms and (2) analyzing which sub-terms are changed after one step of local derandomization. We acknowledge that we have not covered all conditions involved in CO, but we expect that similar ideas would be applicable to some other conditions. See App. F.5 for discussions on some conditions not fully covered in this work, e.g., cycles and trees.

5. Applying the Derivations to CO Problems

In this section, we apply UCOM2 to different CO problems (facility location, maximum coverage, and robust coloring) with both theoretical values, NP-hardness (Mihelic & Robic, 2004; Yanez & Ramirez, 2003), and real-world implications. See App. F for the applications to four more problems (robust k -clique, robust dominating set, clique cover, and minimum spanning tree). Specifically, for each specific problem, we shall (1) check what conditions are involved and (2) construct the probabilistic objective and derandomization process by combining the analyses in Sec. 4, as in the following template.

- (1) Find the conditions involved in the optimization objective ($f = \sum_i f_i$) and the constraints ($X \in \bigcap_i \mathcal{C}_i$).
- (2) Construct the final objective: $\sum_i \tilde{f}_i + \beta \sum_j \tilde{g}_j$ with constraint coefficient $\beta > 0$ by combining the probabilistic functions \tilde{f}_i 's and \tilde{g}_j 's for the optimization objectives and constraints, respectively.

5.1. Facility Location

The *facility location* problem is abstracted from real-world scenarios where the goal is to find some good locations among candidate locations (Drezner & Hamacher, 2004).

Definition. Given (1) a complete weighted graph $G = (V = [n], E = \binom{V}{2}, W)$, where the distance between each pair (u, v) of nodes is $W(u, v) > 0$, and $W(v, v) = 0, \forall v \in V$, and (2) the number k of locations to choose, we aim to find a subset $V_X \subseteq V$ such that (c1) $|V_X| = k$, and (c2) $\sum_{v \in V} \min_{v_X \in V_X} W(v, v_X)$ is minimized.

Involved conditions: (1) cardinality constraints and (2) minimum w.r.t. a subset (see Secs. 4.1 & 4.2).

Details. Given $p \in [0, 1]^n$ and $\beta > 0$,

$$\tilde{f}_{\text{FL}}(p; G, k) = (\sum_{v \in V} \tilde{f}_{\text{ms}}(p; v, W)) + \beta \tilde{f}_{\text{card}}(p; \{k\}).$$

For $i \in [n]$ and $x \in \{0, 1\}$, the ID is $\Delta \tilde{f}_{\text{FL}}(i, x, p; G, k) = \sum_{v \in V} \Delta \tilde{f}_{\text{ms}}(i, x, p; v, W) + \beta \Delta \tilde{f}_{\text{card}}(i, x, p; \{k\})$.

5.2. Maximum Coverage

The *maximum coverage* problem (Khuller et al., 1999) is a classical combinatorial optimization problem with real-world applications including public traffic management (Ali & Dyo, 2017), web management (Saha & Getoor, 2009), and scheduling (Marchiori & Steenbeek, 2000).

Definition. Given (1) m items (WLOG, assume the items are $[m]$), each with weight $W_j, \forall j \in [m]$, (2) a family of n sets $\mathcal{S} = \{S_1, S_2, \dots, S_n\}$ with each $S_i \subseteq [m]$ and (3) the number k of sets to choose, we aim to choose $\mathcal{S}_X \subseteq \mathcal{S}$ from the given sets such that (c1) $|\mathcal{S}_X| = k$, and (c2) the total weights of the covered items $\sum_{j \in T_X} W_j$ is maximized, where $T_X := \bigcup_{S_i \in \mathcal{S}_X} S_i$ is the set of covered items.

Involved conditions: (1) cardinality constraints and (2) covering (see Secs. 4.1 & 4.3).

Details. Construct a bipartite graph $G_{\mathcal{S}} = (V = \mathcal{S} \cup [m], E)$, where $(S_i, j) \in E$ iff $j \in S_i$. For $p \in [0, 1]^n$ and $\beta > 0$,

$$\tilde{f}_{\text{MC}}(p; \mathcal{S}, k) = \sum_{j \in [m]} W_j \tilde{f}_{\text{cv}}(p; j, G_{\mathcal{S}}) + \beta \tilde{f}_{\text{card}}(p; \{k\}).$$

For $i \in [n]$ and $x \in \{0, 1\}$, the ID is $\Delta \tilde{f}_{\text{MC}}(i, x, p; \mathcal{S}, k) = \sum_{j \in [m]} W_j \Delta \tilde{f}_{\text{cv}}(i, x, p; j, G_{\mathcal{S}}) + \beta \Delta \tilde{f}_{\text{card}}(i, x, p; \{k\})$.

5.3. Robust Coloring

The *robust coloring* problem (Yanez & Ramirez, 2003) generalizes the coloring problem (Jensen & Toft, 2011). It is motivated by real-world scheduling problems where some conflicts can be uncertain, with notable applications to supply chain management (Lim & Wang, 2005).

Definition. Given (1) an uncertain graph $G = (V, E, P)$, where $E_h := \{e \in E: P(e) = 1\}$ represents *hard conflicts* which we *must* avoid, and $E_s := \{e \in E: P(e) < 1\}$ are *soft conflicts* which possibly happen, and (2) the number c of colors, we aim to find a c -coloring X on V , where each node $v \in V$ has a color $X_v \in d := \{0, 1, \dots, c-1\}$, such that (c1) no hard conflicts are violated (i.e., $X_u \neq X_v, \forall (u, v) \in E_h$), and (c2) the probability that no violated soft conflicts happen (i.e., $\prod_{e=(u,v) \in E_s: X_u=X_v} (1 - P(e))$) is maximized.

We fix G and c in the analysis below.

Involved conditions: (1) independent sets,¹⁰ (2) uncertainty, and (3) non-binary decisions (see Secs. 4.4 to 4.6).

Details. Regarding (c1), we extend the derivations in Sec. 4.4 to non-binary cases. We use

¹⁰The nodes in each color group should be an independent set.

$$\hat{g}_1(X) := |\{(u, v) \in E_h: X_u = X_v\}|$$

which is a TUB of $g_1(X) := \mathbb{1}(X \notin \mathcal{C}_1)$ with $\mathcal{C}_1 = \{X: (c1) \text{ is satisfied}\}$, and use $\tilde{g}_1(p) := \mathbb{E}_{X \sim p} \hat{g}_1(X)$. Regarding (c2), maximizing $\prod_{e=(u,v) \in E_s: X_u=X_v} (1 - P(e))$ is equivalent to minimizing

$$f_2(X) = - \sum_{e=(u,v) \in E_s: X_u=X_v} \log(1 - P(e)).$$

With $\hat{f}_2(X) := f_2(X)$ and $\tilde{f}_2(p) := \mathbb{E}_{X \sim p} \hat{f}_2(X)$, the final objective is $\tilde{f}_{\text{RC}} = \tilde{f}_2 + \beta \tilde{g}_1$ with constraint coefficient $\beta > 0$.

Lemma 12. \hat{g}_1 is a TUB of g_1 and \hat{f}_2 is a TUB of f_2 .

Proof sketch. We extend the ideas for independent sets in Sec. 4.4, especially Lem. 9. \square

We derive each term in \tilde{f}_{RC} as follows.

Lemma 13. For any $p \in [0, 1]^{n \times c}$, $\tilde{f}_2(p) = \mathbb{E}_{X \sim p} \hat{f}_2(X) = - \sum_{e=(u,v) \in E_s} \sum_{r=0}^{c-1} p_{ur} p_{vr} \log(1 - P(e))$ and $\tilde{g}_1(p) = \mathbb{E}_{X \sim p} \hat{g}_1(X) = \sum_{(u,v) \in E_h} \sum_{r=0}^{c-1} p_{ur} p_{vr}$.

Proof sketch. We extend the ideas in Lem. 10. \square

We then derive the IDs of each term in \tilde{f}_{RC} .

Lemma 14 (IDs of the terms in \tilde{f}_{RC}). For any $p \in [0, 1]^{n \times c}$, $i \in [n]$, and $x \in d$, $\Delta \tilde{g}_1(i, x; p) = \sum_{x' \in d \setminus \{x\}} p_{ix'} \sum_{(i,j) \in E_h} (p_{jx} - p_{jx'})$ and $\Delta \tilde{f}_2(i, x; p) = \sum_{x' \in d \setminus \{x\}} p_{ix'} \sum_{(i,j) \in E_s} (p_{jx'} - p_{jx}) \log(1 - P(i, j))$.

Proof sketch. We extend the ideas in Lem. 11. Changing p_i only affects j with $(i, j) \in E_*$ and we compute the differences for each j . \square

We finally get the overall IDs $\Delta \tilde{f}_{\text{RC}} = \Delta \tilde{f}_2 + \beta \Delta \tilde{g}_1$.

Notes. When practitioners encounter new problems that involve the conditions covered in this work, they can simply combine our derivations for the involved conditions, just as we did in this section. Indeed, we believe many other CO problems involve the conditions considered in this work.

6. Experiments

Through experiments on problems with complex conditions, we shall show the effectiveness of UCOM2.

6.1. Facility Location and Maximum Coverage

We conduct experiments on the facility location problem and the maximum coverage problem (Secs. 5.1 & 5.2). For the experimental settings, we mainly follow an existing work (Wang et al., 2023), with additional datasets and baselines. For fair comparisons, we consider inductive settings (training and test sets are different) and use the same GNN architectures as Wang et al. (2023).¹¹ See App. G.1 for the detailed experimental settings.

¹¹See App. H.1 for discussions on transductive settings.

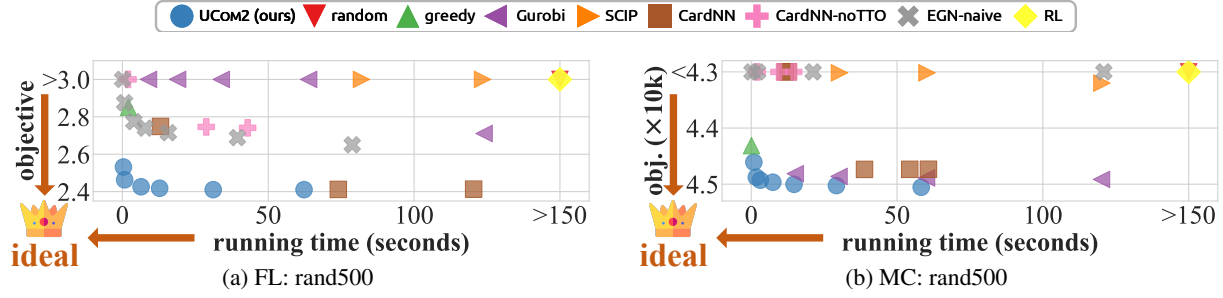


Figure 1: The speed-quality trade-offs on facility location (FL) and maximum coverage (MC). Running time (x -axis): smaller the better. Objective (y -axis): for FL smaller the better; for MC larger the better. For MC, we reverse the y -axis so that the ideal point is always at the bottom left corner. See Fig. 2 in App. G.2 for the results on other datasets.

Table 1: Results on facility location. Running time (time; normalized): smaller the better. Objective (obj; normalized): smaller the better. In each column, ■ indicates ranking 1st, ■ indicates ranking 2nd, and ■ indicates ranking 3rd.

Method	rand500		rand800		starbucks		mcd		subway		average		average rank		
	obj↓	time↓	obj↓	time↓	obj↓	time↓	obj↓	time↓	obj↓	time↓	obj↓	time↓	obj↓	time↓	sum↓
random	1.43	263.29	1.51	125.65	1.86	461.54	1.64	122.45	1.52	119.40	1.61	240.34	11.6	13.6	25.2
greedy	1.19	2.30	1.16	3.08	1.21	12.52	1.19	5.87	1.11	12.94	1.17	7.34	8.6	4.0	12.6
Gurobi	1.07	133.68	1.26	65.47	1.07	197.08	1.51	63.88	2.63	69.08	1.51	105.84	9.0	11.8	20.8
SCIP	1.73	103.55	2.35	100.34	19.76	154.83	55.10	247.91	55.01	366.47	26.79	194.62	15.8	12.8	28.6
CardNN-S	1.14	15.29	1.06	8.45	1.62	36.98	1.16	11.99	1.08	10.14	1.21	16.57	7.4	5.4	12.8
CardNN-GS	1.00	78.38	1.01	74.22	1.07	76.69	1.15	21.60	1.03	14.99	1.05	53.18	4.0	9.0	13.0
CardNN-HGS	1.00	110.14	1.01	95.11	1.07	174.87	1.15	49.20	1.02	28.48	1.05	91.56	3.4	11.2	14.6
CardNN-noTTO-S	1.43	2.23	1.55	1.05	3.34	3.90	3.90	1.00	3.54	1.00	2.75	1.84	14.0	1.6	15.6
CardNN-noTTO-GS	1.14	31.39	1.15	27.18	1.52	15.73	1.26	8.03	1.23	2.21	1.26	16.91	8.8	4.8	13.6
CardNN-noTTO-HGS	1.14	40.97	1.15	32.30	1.45	29.98	1.27	14.44	1.21	3.67	1.24	24.27	8.4	6.6	15.0
EGN-naive	1.10	86.45	1.14	44.66	1.14	232.44	1.66	24.53	1.47	60.13	1.30	89.64	8.6	10.6	19.2
RL-transductive	2.32	329.11	2.24	157.07	10.24	3461.54	2.77	918.37	2.51	895.52	4.02	1152.32	14.6	15.6	30.2
RL-inductive	1.70	329.17	1.85	157.35	2.72	577.00	2.55	153.08	2.36	149.28	2.24	273.18	13.2	15.0	28.2
UCOM2-short	1.05	1.00	1.03	1.00	1.03	1.00	1.05	1.31	1.04	1.77	1.04	1.89	4.2	1.4	5.6
UCOM2-middle	1.00	32.56	1.00	15.65	1.03	4.35	1.01	4.47	1.01	13.05	1.01	14.02	2.0	4.8	6.8
UCOM2-long	1.00	81.03	1.00	31.12	1.00	20.27	1.00	19.41	1.00	22.88	1.00	34.94	1.0	7.8	8.8

Table 2: Results on maximum coverage. Running time (time; normalized): smaller the better. Objective (obj; normalized): larger the better. In each column, ■ indicates ranking 1st, ■ indicates ranking 2nd, and ■ indicates ranking 3rd.

Method	rand500		rand1000		twitich		railway		average		average rank		
	obj↑	time↓	obj↑	time↓	obj↑	time↓	obj↑	time↓	obj↑	time↓	obj↑	time↓	sum↓
random	0.82	2666.67	0.79	727.27	0.52	369.23	0.96	315.79	0.77	1019.74	12.8	14.0	26.8
greedy	0.98	1.00	0.99	1.00	1.00	1.06	1.00	1.00	0.99	1.02	7.3	1.3	8.5
Gurobi	1.00	1333.89	1.00	363.94	1.00	1.00	1.00	158.87	1.00	464.42	3.3	8.8	12.0
SCIP	0.97	1334.11	0.96	362.09	1.00	5.05	1.00	159.84	0.98	465.27	6.3	10.8	17.0
CardNN-S	0.93	130.33	0.93	35.94	1.00	12.25	0.97	3.71	0.96	45.56	8.0	5.5	13.5
CardNN-GS	0.99	448.11	1.00	169.55	1.00	25.38	1.00	23.21	1.00	166.56	4.3	9.0	13.3
CardNN-HGS	0.99	618.22	1.00	248.33	1.00	47.28	1.00	35.86	1.00	237.42	3.3	10.5	13.8
CardNN-noTTO-S	0.70	20.33	0.69	6.18	0.01	1.43	0.94	1.54	0.58	7.37	16.0	2.8	18.8
CardNN-noTTO-GS	0.82	115.56	0.79	61.18	0.02	2.97	0.96	7.53	0.65	46.81	13.5	5.0	18.5
CardNN-noTTO-HGS	0.82	132.56	0.79	75.15	0.19	3.62	0.96	12.14	0.69	55.87	12.3	6.5	18.8
EGN-naive	0.92	1334.56	0.91	364.45	0.13	185.22	0.97	159.13	0.73	510.84	11.3	12.8	24.0
RL-transductive	0.92	3333.33	0.82	909.09	0.95	2769.23	0.96	2368.42	0.91	2345.02	11.5	15.5	27.0
RL-inductive	0.77	3334.00	0.77	909.64	0.59	464.48	0.96	397.08	0.77	1276.30	13.8	15.5	29.3
UCOM2-short	0.99	10.67	0.99	5.55	1.00	2.80	1.00	2.63	1.00	5.41	5.8	2.8	8.5
UCOM2-middle	1.00	168.44	1.00	23.76	1.00	17.58	1.00	10.75	1.00	55.13	3.8	6.5	10.3
UCOM2-long	1.00	333.56	1.00	222.85	1.00	29.77	1.00	21.11	1.00	151.82	2.3	9.0	11.3

Methods. We compare UCOM2 with: (1) **random**: k locations or sets are picked uniformly at random; (2) **greedy**: deterministic greedy algorithms; (3-4) **Gurobi** (Gurobi Optimization, LLC, 2023) and **SCIP** (Bestuzheva et al., 2021; Perron & Furnon, 2023): the problems are formulated as MIPs and the two solvers are used; (5) **CardNN** (Wang et al., 2023): a SOTA UL4CO method with three variants; (6) **CardNN-noTTO**: CardNN directly optimizes on each test graph in test time, and these are variants of CardNN without test-time optimization; (7) **EGN-naive**: EGN (Kar-

alias & Loukas, 2020) with a naive probabilistic objective construction and iterative rounding; (8) **RL**: a reinforcement-learning method (Kool et al., 2019).¹²

Datasets. We consider both synthetic and real-world graphs.

- **Random graphs:** The number after “rand” represents the size of the random graphs. Each group of random graphs contains 100 graphs from the same distribution.

¹²See App. H.2 for discussions on reinforcement learning.

Table 3: Results on robust coloring. Running time (time; in seconds): smaller the better. Objective (obj): smaller the better. In each column, ■ indicates ranking 1st, and ■ indicates ranking 2nd.

Method	collins, 18 colors		collins, 25 colors		gavin, 8 colors		gavin, 15 colors		krogan, 8 colors		krogan, 15 colors		ppi, 47 colors		ppi, 50 colors		average rank		
	obj↓	time↓	obj↓	time↓	obj↓	time↓	obj↓	time↓	obj↓	time↓	obj↓	time↓	obj↓	time↓	obj↓	time↓	obj↓	time↓	sum↓
greedy-RD	115.33	300.34	23.42	300.79	66.51	300.53	7.36	301.46	117.47	300.06	0.87	301.24	4.16	301.31	1.23	301.24	2.88	3.25	6.13
greedy-GA	114.36	188.21	22.20	243.93	66.51	398.90	7.36	540.62	117.47	941.35	0.87	1256.66	3.66	1416.38	1.23	1484.27	2.50	4.25	6.75
DC	586.56	300.28	159.15	300.38	311.91	300.11	58.10	300.12	1065.52	300.07	1.76	300.46	43.35	300.13	6.72	300.76	5.00	2.50	7.50
Gurobi	87.28	301.71	16.23	306.10	42.41	300.80	7.28	303.50	46.78	300.80	0.87	51.70	4.60	328.48	1.31	313.23	2.50	4.00	6.50
UCOM2 (CPU)	82.26	79.36	15.16	54.37	42.99	152.20	260.90	17.25	211.43	13.73	0.87	8.55	2.93	116.54	1.01	120.56	1.50	1.00	2.50
UCOM2 (GPU)	82.26	7.09	15.16	8.03	42.99	13.28	6.72	17.25	53.44	13.73	0.87	1.91	2.93	5.24	1.01	5.48	1.50	1.00	2.50

• **Real-world graphs:** For facility location, each graph contains real-world entities with locations (*starbucks*, *mcd*, *subway*). For maximum coverage, each graph contains real-world sets (*twitch*, *railway*). Each group of real-world graphs contains multiple graphs from the same source.

Speed-quality trade-offs. For several methods (including UCOM2), we can grant more running time to obtain better optimization quality. For UCOM2, we use test-time augmentation (Jin et al., 2023) on the test graphs by adding perturbations into graph topology and features. Three variants of UCOM2 use different numbers of augmented data.

Evaluation. For each group of datasets and each method, we report the average optimization objective and running time over five trials. We also report the overall objective, time, and ranks, averaged over all the groups of datasets. The average rank “sum” (ARS) is the summation of the average ranks w.r.t. objective and time. See App. G for the full results with standard deviations and ablation studies.

Results. On both problems, UCOM2 achieves the best trade-offs overall (Tabs. 1 & 2). On facility location, the top-3 methods w.r.t. ARS are the three variants of UCOM2. On maximum coverage, the three variants rank 1, 3, and 4 w.r.t. ARS, respectively. In Fig. 1, we report the detailed trade-offs of different methods on the random graphs, visually illustrating the best trade-off overall by UCOM2.

6.2. Robust Coloring

We conduct experiments on the robust coloring problem (see Sec. 5.3) under transductive settings directly optimizing probabilistic decisions p . See App. G.1 for more details.

Methods. We compare UCOM2 with four baseline methods. (1-2) **Greedy-RD** and **greedy-GA**: both methods decide the colors following an enumeration of nodes, where greedy-RD follows a random (RD) permutation of the nodes while greedy-GA uses a genetic algorithm (GA) to learn the permutation;¹³ (3) **Deterministic coloring (DC)**: a deterministic greedy coloring algorithm (Kosowski & Manuszewski, 2004) is used to avoid all the hard conflicts, and it tries to avoid as many soft conflicts as possible; (4) **Gurobi**: the problem is formulated as an MIP and the solver is used.

¹³Greedy-GA is the method proposed by Yanez & Ramirez (2003) in the original paper of robust coloring.

Datasets. We use four real-world uncertain graphs: (1) **collins**, (2) **gavin**, (3) **krogan**, and (4) **PPI**.

Speed-quality trade-offs. We record the running time of UCOM2 using only CPUs and using GPUs. For UCOM2, we use multiple initial probabilities. We make sure that even with only CPUs, UCOM2 uses less time than each baseline.

Evaluation. For each group of datasets and each method, we report the average optimization objective and running time over five trials. The average ranks are computed in the same way as for facility location and maximum coverage.

Ablation studies. We analyze different components in UCOM2 and show that (1) good probabilistic objectives are helpful, (2) greedy derandomization is more effective than iterative rounding, and (3) incremental derandomization improves the speed. See App. G.3 for more details.

Results. As shown in Tab. 3, with the least running time, UCOM2 consistently achieves (1) better optimization quality than the two **greedy** baselines and **DC** and (2) better optimization quality than **Gurobi** in most cases. This superiority holds even when we only use CPUs for UCOM2. When using GPUs, UCOM2 is even faster.

7. Conclusion

In this work, we study and propose UCOM2 (**U**nsupervised **C**ombinatorial Optimization Under **C**omplex Conditions). Specifically, we concretize the targets for probabilistic objective construction and derandomization (Sec. 3) with theoretical justification (Thms. 1 and 2), derive non-trivial objectives and derandomization for various complex conditions (e.g., cardinality constraints, minimum, and covering) to meet the targets (Sec. 4; Lems. 1 to 11), apply the derivations to different problems involving such conditions (Sec. 5), and finally show the empirical superiority of our method via extensive experiments (Sec. 6). For reproducibility, we share the code and datasets online (Anonymous, 2024).

Discussion. As discussed in Sec. 4, we have not covered all conditions involved in CO in this work, while we believe that our high-level ideas are applicable to other conditions and problems. The performance of UCOM2 and general UL4CO on hard instances (Xu et al., 2007; Xu & Zhou, 2023) is an interesting topic for future exploration.

Potential Broader Impact

This paper presents work whose goal is to advance the field of Machine Learning, especially Machine Learning for Combinatorial Optimization. There are many potential societal consequences of our work, none of which we feel must be specifically highlighted here.

References

- Ahn, S., Seo, Y., and Shin, J. Learning what to defer for maximum independent sets. In *ICML*, 2020.
- Ali, J. and Dyo, V. Coverage and mobile sensor placement for vehicles on predetermined routes: A greedy heuristic approach. In *WINSYS*, 2017.
- Alon, N. and Spencer, J. H. *The probabilistic method*. John Wiley & Sons, 2016.
- Anonymous. Tackling complex conditions in unsupervised combinatorial optimization: Code and datasets. <https://anonymous.4open.science/r/ucom2-D168>, 2024.
- Aramon, M., Rosenberg, G., Valiante, E., Miyazawa, T., Tamura, H., and Katzgraber, H. G. Physics-inspired optimization for quadratic unconstrained problems using a digital annealer. *Frontiers in Physics*, 7:48, 2019.
- Bach, F. et al. Learning with submodular functions: A convex optimization perspective. *Foundations and Trends® in machine learning*, 6(2-3):145–373, 2013.
- Bello, I., Pham, H., Le, Q. V., Norouzi, M., and Bengio, S. Neural combinatorial optimization with reinforcement learning. In *ICLR*, 2016.
- Bengio, Y., Lodi, A., and Prouvost, A. Machine learning for combinatorial optimization: a methodological tour d’horizon. *European Journal of Operational Research*, 290(2):405–421, 2021.
- Berthet, Q., Blondel, M., Teboul, O., Cuturi, M., Vert, J.-P., and Bach, F. Learning with differentiable perturbed optimizers. In *NeurIPS*, 2020.
- Berto, F., Hua, C., Park, J., Kim, M., Kim, H., Son, J., Kim, H., Kim, J., and Park, J. R14co: an extensive reinforcement learning for combinatorial optimization benchmark. *arXiv:2306.17100*, 2023.
- Bestuzheva, K., Besançon, M., Chen, W.-K., Chmiela, A., Donkiewicz, T., van Doornmalen, J., Eifler, L., Gaul, O., Gamrath, G., Gleixner, A., et al. The scip optimization suite 8.0. *arXiv preprint arXiv:2112.08872*, 2021.
- Billionnet, A. Different formulations for solving the heaviest k-subgraph problem. *INFOR: Information Systems and Operational Research*, 43(3):171–186, 2005.
- Bomze, I. M., Budinich, M., Pardalos, P. M., and Pelillo, M. The maximum clique problem. *Handbook of Combinatorial Optimization: Supplement Volume A*, pp. 1–74, 1999.
- Buchbinder, N., Feldman, M., Naor, J., and Schwartz, R. Submodular maximization with cardinality constraints. In *SODA*, 2014.
- Cappart, Q., Chételat, D., Khalil, E. B., Lodi, A., Morris, C., and Velickovic, P. Combinatorial optimization and reasoning with graph neural networks. *J. Mach. Learn. Res.*, 24:130–1, 2023.
- Caprara, A., Toth, P., and Fischetti, M. Algorithms for the set covering problem. *Annals of Operations Research*, 98(1-4):353–371, 2000.
- Ceccarello, M., Fantozzi, C., Pietracaprina, A., Pucci, G., and Vandin, F. Clustering uncertain graphs. In *PVLDB*, 2017.
- Ceria, S., Nobili, P., and Sassano, A. A lagrangian-based heuristic for large-scale set covering problems. *Mathematical Programming*, 81:215–228, 1998.
- Chalumeau, F., Surana, S., Bonnet, C., Grinsztajn, N., Pretorius, A., Alexandre, L., and Barrett, T. Combinatorial optimization with policy adaptation using latent space search. In *NeurIPS*, 2023.
- Chen, X., Chen, M., Shi, W., Sun, Y., and Zaniolo, C. Embedding uncertain knowledge graphs. In *AAAI*, 2019.
- Choo, J., Kwon, Y.-D., Kim, J., Jae, J., Hottung, A., Tierney, K., and Gwon, Y. Simulation-guided beam search for neural combinatorial optimization. In *NeurIPS*, 2022.
- Delarue, A., Anderson, R., and Tjandraatmadja, C. Reinforcement learning with combinatorial actions: An application to vehicle routing. In *NeurIPS*, 2020.
- Diaby, M. The traveling salesman problem: a linear programming formulation. *arXiv preprint cs/0609005*, 2006.
- Drakulic, D., Michel, S., Mai, F., Sors, A., and Andreoli, J.-M. Bq-nco: Bisimulation quotienting for generalizable neural combinatorial optimization. In *NeurIPS*, 2023.
- Drezner, Z. and Hamacher, H. W. *Facility location: applications and theory*. Springer Science & Business Media, 2004.
- Erdős, P. and Spencer, J. *Probabilistic methods in combinatorics*. Akadémiai Kiadó, 1974.
- Feige, U., Peleg, D., and Kortsarz, G. The dense k-subgraph problem. *Algorithmica*, 29:410–421, 2001.

- Ferber, A. M., Huang, T., Zha, D., Schubert, M., Steiner, B., Dilkina, B., and Tian, Y. Surco: Learning linear surrogates for combinatorial nonlinear optimization problems. In *ICML*, 2023.
- Graham, R. L. and Hell, P. On the history of the minimum spanning tree problem. *Annals of the History of Computing*, 7(1):43–57, 1985.
- Gramm, J., Guo, J., Hüffner, F., and Niedermeier, R. Data reduction and exact algorithms for clique cover. *Journal of Experimental Algorithmics (JEA)*, 13:2–2, 2009.
- Grinsztajn, N., Daniel, F.-B., Shikha, S., Bonnet, C., and Barrett, T. Winner takes it all: Training performant rl populations for combinatorial optimization. In *NeurIPS*, 2023.
- Guha, S. and Khuller, S. Approximation algorithms for connected dominating sets. *Algorithmica*, 20:374–387, 1998.
- Gurobi Optimization, LLC. Gurobi Optimizer Reference Manual, 2023. URL <https://www.gurobi.com>.
- Hong, Y. On computing the distribution function for the poisson binomial distribution. *Computational Statistics & Data Analysis*, 59:41–51, 2013.
- Hu, J., Cheng, R., Huang, Z., Fang, Y., and Luo, S. On embedding uncertain graphs. In *CIKM*, 2017.
- Jensen, T. R. and Toft, B. *Graph coloring problems*. John Wiley & Sons, 2011.
- Jin, W., Zhao, T., Ding, J., Liu, Y., Tang, J., and Shah, N. Empowering graph representation learning with test-time graph transformation. In *ICLR*, 2023.
- Karalias, N. and Loukas, A. Erdos goes neural: an unsupervised learning framework for combinatorial optimization on graphs. In *NeurIPS*, 2020.
- Karalias, N., Robinson, J., Loukas, A., and Jegelka, S. Neural set function extensions: Learning with discrete functions in high dimensions. In *NeurIPS*, 2022.
- Khalil, E., Dai, H., Zhang, Y., Dilkina, B., and Song, L. Learning combinatorial optimization algorithms over graphs. In *NeurIPS*, 2017.
- Khuller, S., Moss, A., and Naor, J. S. The budgeted maximum coverage problem. *Information processing letters*, 70(1):39–45, 1999.
- Kim, M., Park, J., et al. Learning collaborative policies to solve np-hard routing problems. In *NeurIPS*, 2021.
- Kim, M., Park, J., and Park, J. Sym-nco: Leveraging symmetricity for neural combinatorial optimization. In *NeurIPS*, 2022.
- Kollovieh, M., Charpentier, B., Zügner, D., and Günnemann, S. Expected probabilistic hierarchies, 2024. URL <https://openreview.net/forum?id=Q3FoelfDjh>.
- Kool, W., Van Hoof, H., and Welling, M. Attention, learn to solve routing problems! In *ICLR*, 2019.
- Kosowski, A. and Manuszewski, K. Classical coloring of graphs. *Contemporary Mathematics*, 352:1–20, 2004.
- Lachapelle, S., Brouillard, P., Deleu, T., and Lacoste-Julien, S. Gradient-based neural dag learning. In *ICLR*, 2020.
- Li, Y., Guo, J., Wang, R., and Yan, J. From distribution learning in training to gradient search in testing for combinatorial optimization. In *NeurIPS*, 2023.
- Lim, A. and Wang, F. Robust graph coloring for uncertain supply chain management. In *HICSS*, 2005.
- Luo, F., Lin, X., Liu, F., Zhang, Q., and Wang, Z. Neural combinatorial optimization with heavy decoder: Toward large scale generalization. In *NeurIPS*, 2023.
- Marchiori, E. and Steenbeek, A. An evolutionary algorithm for large scale set covering problems with application to airline crew scheduling. In *Workshops on Real-World Applications of Evolutionary Computation*, 2000.
- Mazyavkina, N., Sviridov, S., Ivanov, S., and Burnaev, E. Reinforcement learning for combinatorial optimization: A survey. *Computers & Operations Research*, 134: 105400, 2021.
- Mihelic, J. and Robic, B. Facility location and covering problems. In *Proc. of the 7th International Multiconference Information Society*, volume 500, 2004.
- Min, Y., Bai, Y., and Gomes, C. P. Unsupervised learning for solving the travelling salesman problem. In *NeurIPS*, 2023.
- Miryoosefi, S. and Jin, C. A simple reward-free approach to constrained reinforcement learning. In *ICML*, 2022.
- Munikoti, S., Agarwal, D., Das, L., Halappanavar, M., and Natarajan, B. Challenges and opportunities in deep reinforcement learning with graph neural networks: A comprehensive review of algorithms and applications. *IEEE Transactions on Neural Networks and Learning Systems*, 2023.
- Nazari, M., Oroojlooy, A., Snyder, L., and Takác, M. Reinforcement learning for solving the vehicle routing problem. In *NeurIPS*, 2018.

- Papp, P. A., Martinkus, K., Faber, L., and Wattenhofer, R. Dropgnn: Random dropouts increase the expressiveness of graph neural networks. In *NeurIPS*, 2021.
- Paulus, A., Rolínek, M., Musil, V., Amos, B., and Martius, G. Combopnet: Fit the right np-hard problem by learning integer programming constraints. In *ICML*, 2021.
- Perron, L. and Furnon, V. Or-tools v9.7, 2023. URL <https://developers.google.com/optimization/>.
- Pettie, S. and Ramachandran, V. An optimal minimum spanning tree algorithm. *Journal of the ACM (JACM)*, 49(1):16–34, 2002.
- Pogancic, M. V., Paulus, A., Musil, V., Martius, G., and Rolinek, M. Differentiation of blackbox combinatorial solvers. In *ICLR*, 2019.
- Qiu, R., Sun, Z., and Yang, Y. Dimes: A differentiable meta solver for combinatorial optimization problems. In *NeurIPS*, 2022.
- Rozemberczki, B., Allen, C., and Sarkar, R. Multi-scale attributed node embedding. *Journal of Complex Networks*, 9(2):cnab014, 2021.
- Saha, B. and Getoor, L. On maximum coverage in the streaming model & application to multi-topic blog-watch. In *SDM*, 2009.
- Sanokowski, S., Berghammer, W., Hochreiter, S., and Lehner, S. L. Variational annealing on graphs for combinatorial optimization. In *NeurIPS*, 2023.
- Schuetz, M. J., Brubaker, J. K., and Katzgraber, H. G. Combinatorial optimization with physics-inspired graph neural networks. *Nature Machine Intelligence*, 4(4):367–377, 2022a.
- Schuetz, M. J., Brubaker, J. K., Zhu, Z., and Katzgraber, H. G. Graph coloring with physics-inspired graph neural networks. *Physical Review Research*, 4(4):043131, 2022b.
- Shu, J., Xi, B., Li, Y., Wu, F., Kamhoua, C., and Ma, J. Understanding dropout for graph neural networks. In *TheWebConf (WWW)*, 2022.
- Sinkhorn, R. and Knopp, P. Concerning nonnegative matrices and doubly stochastic matrices. *Pacific Journal of Mathematics*, 21(2):343–348, 1967.
- Son, J., Kim, M., Kim, H., and Park, J. Meta-sage: Scale meta-learning scheduled adaptation with guided exploration for mitigating scale shift on combinatorial optimization. In *ICML*, 2023.
- Straka, M. Poisson binomial distribution for python (github repository). <https://github.com/tsakim/poibin>, 2017.
- Sun, H., Goshvadi, K., Nova, A., Schuurmans, D., and Dai, H. Revisiting sampling for combinatorial optimization. In *ICML*, 2023.
- Sun, Z. and Yiming, Y. Difusco: Graph-based diffusion solvers for combinatorial optimization. In *NeurIPS*, 2023.
- Viquerat, J., Duvigneau, R., Meliga, P., Kuhnle, A., and Hachem, E. Policy-based optimization: Single-step policy gradient method seen as an evolution strategy. *Neural Computing and Applications*, 35(1):449–467, 2023.
- Wang, H. and Li, P. Unsupervised learning for combinatorial optimization needs meta-learning. In *ICLR*, 2023.
- Wang, H. P., Wu, N., Yang, H., Hao, C., and Li, P. Unsupervised learning for combinatorial optimization with principled objective relaxation. In *NeurIPS*, 2022.
- Wang, R., Shen, L., Chen, Y., Yang, X., Tao, D., and Yan, J. Towards one-shot neural combinatorial solvers: Theoretical and empirical notes on the cardinality-constrained case. In *ICLR*, 2023.
- Wang, Y. H. On the number of successes in independent trials. *Statistica Sinica*, pp. 295–312, 1993.
- Xu, K. and Zhou, G. Sat requires exhaustive search. *arXiv preprint arXiv:2302.09512*, 2023.
- Xu, K., Boussemart, F., Hemery, F., and Lecoutre, C. Random constraint satisfaction: Easy generation of hard (satisfiable) instances. *Artificial intelligence*, 171(8-9):514–534, 2007.
- Yanez, J. and Ramirez, J. The robust coloring problem. *European Journal of Operational Research*, 148(3):546–558, 2003.
- Yannakakis, M. Expressing combinatorial optimization problems by linear programs. In *Proceedings of the twentieth annual ACM symposium on Theory of computing*, pp. 223–228, 1988.
- Ye, H., Wang, J., Cao, Z., Liang, H., and Li, Y. Deepaco: Neural-enhanced ant systems for combinatorial optimization. In *NeurIPS*, 2023a.
- Ye, X., Yan, G., and Yan, J. Towards quantum machine learning for constrained combinatorial optimization: a quantum qap solver. In *ICML*, 2023b.
- Zhang, D., Dai, H., Malkin, N., Courville, A., Bengio, Y., and Pan, L. Let the flows tell: Solving graph combinatorial optimization problems with flownets. In *NeurIPS*, 2023.

Zhong, C., Malinen, M., Miao, D., and Fränti, P. A fast minimum spanning tree algorithm based on k-means. *Information Sciences*, 295:1–17, 2015.

A. Proofs

Here, we provide proof for each theoretical statement in the main text.

Theorem 1 (Expectations are all you need). *For any $g : \{0, 1\}^n \rightarrow \mathbb{R}$, $\tilde{g} : [0, 1]^n \rightarrow \mathbb{R}$ with $\tilde{g}(p) = \mathbb{E}_{X \sim p} g(X)$ is differentiable and entry-wise concave w.r.t. p .*

Proof. For any p and i , we have

$$\begin{aligned}
 \tilde{g}(p) &= \mathbb{E}_{X \sim p} g(X) \\
 &= \sum_{X \in \{0, 1\}^n} \Pr_p[X] g(X) \\
 &= \sum_X \prod_{v \in V_X} p_v \prod_{u \in [n] \setminus V_X} (1 - p_u) g(X) \\
 &= \sum_{X: i \in V_X} \left(\prod_{v \in V_X, v \neq i} p_v \prod_{u \in [n] \setminus V_X} (1 - p_u) \right) p_i g(X) + \sum_{X: i \notin V_X} \left(\prod_{v \in V_X} p_v \prod_{u \in [n] \setminus V_X, u \neq i} (1 - p_u) \right) (1 - p_i) g(X) \\
 &= p_i \sum_{X: i \in V_X} \prod_{v \in V_X, v \neq i} p_v \prod_{u \in [n] \setminus V_X} (1 - p_u) g(X) + (1 - p_i) \sum_{X: i \notin V_X} \prod_{v \in V_X} p_v \prod_{u \in [n] \setminus V_X, u \neq i} (1 - p_u) g(X) \\
 &= p_i \tilde{g}(\text{der}(i, 1; p)) + (1 - p_i) \tilde{g}(\text{der}(i, 0; p)) \\
 &\geq p_i \tilde{g}(\text{der}(i, 1; p)) + (1 - p_i) \tilde{g}(\text{der}(i, 0; p)),
 \end{aligned}$$

completing the proof on entry-wise concavity. Regarding differentiability, since

$$\mathbb{E}_{X \sim p} g(X) = \sum_{X \in \{0, 1\}^n} \Pr_p[X] g(X),$$

it suffices to show that

$$\Pr_p[X] g(X) = \prod_{v \in V_X} p_v \prod_{u \in [n] \setminus V_X} (1 - p_u) g(X)$$

is differentiable w.r.t p for each $X \in \{0, 1\}^n$. Indeed, fix any X , $\prod_{v \in V_X} p_v \prod_{u \in [n] \setminus V_X} (1 - p_u) g(X)$ is a polynomial of p_i 's, and is thus differentiable w.r.t. p . \square

Theorem 2 (Goodness of greedy derandomization). *For any entry-wise concave \tilde{f} and any $p_o \in [0, 1]^n$, the above process of greedy derandomization can always reach a point where the final p_{final} is **(G1)** discrete (i.e., $p_{\text{final}} \in \{0, 1\}^n$), **(G2)** no worse than p_o (i.e., $\tilde{f}(p_{\text{final}}) \leq \tilde{f}(p_o)$), and **(G3)** a local minimum (i.e., $\tilde{f}(p_{\text{final}}) \leq \min_{(i, x) \in [n] \times \{0, 1\}} \tilde{f}(\text{der}(i, x; p_{\text{final}}))$).*

Proof of Theorem 2. First, we claim that for any non-discrete $p_{\text{cur}} \notin \{0, 1\}^n$, we can always derandomize it through a series of local derandomization while the value of \tilde{f} does not increase. This is guaranteed by the entry-wise concavity of \tilde{f} . Specifically, since

$$p_i \tilde{f}(\text{der}(i, 1; p)) + (1 - p_i) \tilde{f}(\text{der}(i, 0; p)) \leq \tilde{f}(p), \forall p, i,$$

we have

$$\min(\text{der}(i, 1; p), \text{der}(i, 0; p)) \leq \tilde{f}(p), \forall p, i,$$

which implies that we can always derandomize a non-discrete entry without increasing the value of \tilde{f} . Therefore, if we greedily improve \tilde{f} via local derandomization, we can always terminate at a discrete point, completing the proof for point (G1). Point (G2) holds since at each step we make sure that the value of \tilde{f} does not increase. Point (G3) holds from the way we conduct local derandomization. Specifically, if the current p_{cur} is not a local minimum, we can always find a possible local derandomization step to proceed with the process while strictly decreasing the value of \tilde{f} . \square

Lemma 1. \hat{f}_{card} is a tight upper bound of $\mathbb{1}[|V_X| \notin C_c]$.

Proof. When $X \notin C_c$, $|V_X| \neq k$, $\forall k \in C_c$, and thus $\hat{f}_{\text{card}}(X; C_c) = \min_{k \in C_c} ||V_X| - k| > 0$ and thus $\hat{f}_{\text{card}}(X; C_c) \geq 1$ since $|V_X| \neq k$ is an integer. When $X \in C_c$, $\exists k \in C_c$, $|V_X| = k$ and thus $\hat{f}_{\text{card}}(X; C_c) = \min_{k \in C_c} ||V_X| - k| = 0$. \square

Lemma 2 (IDs of \tilde{f}_{card}). For any p, i, t , let $q_s := \Pr_{X \sim p}[|V_X| = s]$ and $q'_s := \Pr_{X \sim p}[|V_X \setminus \{i\}| = s]$, $\forall s$,

$$\begin{aligned} q'_t &= (1 - p_i)^{-1} \sum_{s=0}^t q_s \left(\frac{p_i}{p_i - 1} \right)^{t-s} \quad (\text{if } p_i \neq 1) \\ &= (p_i)^{-1} \sum_{s=0}^{n-t-1} q_{t+s+1} \left(\frac{p_i - 1}{p_i} \right)^s \quad (\text{if } p_i \neq 0). \end{aligned}$$

Based on that,

$$\begin{cases} \Delta \tilde{f}_{\text{card}}(i, 0, p; C_c) = \sum_{t \in [n] \setminus C_c} (q'_t - q_t) \min_{k \in C_c} |t - k|, \\ \Delta \tilde{f}_{\text{card}}(i, 1, p; C_c) = \sum_{t \in [n] \setminus C_c} (q'_{t-1} - q_t) \min_{k \in C_c} |t - k|. \end{cases}$$

Proof. Fix any $i \in [n]$ and any $p \in [0, 1]^n$, we have

$$\begin{cases} \Pr_{X \sim p}[|V_X| = 0] = \Pr_{X \sim p}[|V_X \setminus \{i\}| = 0](1 - p_i) \\ \Pr_{X \sim p}[|V_X| = t] = \Pr_{X \sim p}[|V_X \setminus \{i\}| = t](1 - p_i) + \Pr_{X \sim p}[|V_X \setminus \{i\}| = t - 1]p_i, \forall t \\ \Pr_{X \sim p}[|V_X| = n] = \Pr_{X \sim p}[|V_X \setminus \{i\}| = n - 1]p_i \end{cases} \quad (3)$$

Let q_s denote $\Pr_{X \sim p}[|V_X| = s]$ for each s as in the statement, and also let \tilde{q}_s denote $\Pr_{X \sim p}[|V_X \setminus \{i\}| = s]$. By Equation (3), if we start from $q_0 = \tilde{q}_0(1 - p_i)$, we have

$$\tilde{q}_0 = \frac{q_0}{1 - p_i}, \tilde{q}_1 = \frac{q_1 - p_i \tilde{q}_0}{1 - p_i} = \frac{q_1(1 - p_i) - q_0 p_i}{(1 - p_i)^2}, \dots,$$

which satisfies $\tilde{q}_t = (1 - p_i)^{-1} \sum_{s=0}^t q_s \left(\frac{p_i}{p_i - 1} \right)^{t-s}$. Now, if

$$\tilde{q}_t = (1 - p_i)^{-1} \sum_{s=0}^t q_s \left(\frac{p_i}{p_i - 1} \right)^{t-s}$$

holds for all $t \leq T - 1$, we aim to show that it also holds for $t = T$, which shall prove the statement by mathematical induction. Indeed, we have

$$\tilde{q}_T = \frac{q_T - p_i \tilde{q}_{T-1}}{1 - p_i} = \frac{q_T - p_i(1 - p_i)^{-1} \sum_{s=0}^{T-1} q_s \left(\frac{p_i}{p_i - 1} \right)^{T-1-s}}{1 - p_i} = (1 - p_i)^{-1} \sum_{s=0}^T q_s \left(\frac{p_i}{p_i - 1} \right)^{T-s},$$

completing the proof. If we start from $q_n = \tilde{q}_{n-1}p_i$, we can obtain the another term (i.e., $(p_i)^{-1} \sum_{s=0}^{n-t-1} q_{t+s+1} \left(\frac{p_i - 1}{p_i} \right)^s$) in the statement in a similar way.

In practice, we use $(1 - p_i)^{-1} \sum_{s=0}^t q_{t-s} \left(\frac{p_i}{p_i - 1} \right)^{t-s}$ for $0 \leq p_i \leq 0.5$ and $(p_i)^{-1} \sum_{s=0}^{n-t-1} q_{t+s+1} \left(\frac{p_i - 1}{p_i} \right)^s$ for $0.5 < p_i \leq 1$, which results in higher numerical stability. \square

Lemma 3. \hat{f}_{ms} is a tight upper bound of f_{ms} .

Proof. As mentioned in Rem. 2, since $\hat{f}_{\text{ms}} = f_{\text{ms}}$, \hat{f} is a tight upper bound of f_{ms} . \square

Lemma 4. For any $p \in [0, 1]^n$, $\mathbb{E}_{X \sim p} \hat{f}_{\text{ms}}(X; i, h) = p_{v_1} d_1 + (1 - p_{v_1}) p_{v_2} d_2 + \dots + (\prod_{j=1}^{n-1} (1 - p_{v_j})) p_{v_n} d_n$.

Proof. By the definition of expectation,

$$\mathbb{E}_{X \sim p} \hat{f}_{\text{ms}}(X; i, h) = \sum_t \Pr[\min_{v_X \in V_X} h(i, v_X) = d_t] d_t,$$

where $\min_{v_X \in V_X} h(i, v_X) = d_t$ if and only if $v_{t'} \notin V_x$ for each $t' < t$ and $v_t \in V_x$, which has probability $(\prod_{j=1}^{t-1} (1 - p_{v_j})) p_{v_t}$. Hence,

$$\mathbb{E}_{X \sim p} \hat{f}_{\text{ms}}(X; i, h) = p_{v_1} d_1 + (1 - p_{v_1}) p_{v_2} d_2 + \dots + (\prod_{j=1}^{n-1} (1 - p_{v_j})) p_{v_n} d_n.$$

\square

Lemma 5 (IDs of \tilde{f}_{ms}). For any $p \in [0, 1]^n$ and $j \in [n]$, let $q_j := (\prod_{k=1}^{j-1} (1 - p_{v_k})) p_{v_j}$, the coefficient of d_j in \tilde{f}_{ms} . Then

$$\begin{cases} \Delta \tilde{f}_{\text{ms}}(v_j, 0, p; i, h) = -q_j d_j + \frac{p_{v_j}}{1 - p_{v_j}} \sum_{j' > j} q_{j'} d_{j'}, \\ \Delta \tilde{f}_{\text{ms}}(v_j, 1, p; i, h) = \sum_{j' > j} q_{j'} (d_j - d_{j'}). \end{cases}$$

Proof. When $p' = \text{der}(v_j, 0; p)$, we have

$$\begin{aligned} \tilde{f}_{\text{ms}}(p'; i, h) &= p'_{v_1} d_1 + (1 - p'_{v_1}) p'_{v_2} d_2 + \cdots + (\prod_{s=1}^{n-1} (1 - p'_{v_s})) p'_{v_n} d_n \\ &= \sum_{s < j} \prod_{k=1}^{s-1} (1 - p_{v_k}) p_{v_s} d_s + 0 + \sum_{t > j} \prod_{1 \leq k \leq t-1, k \neq j} (1 - p_{v_k}) p_{v_t} d_t \\ &= \sum_{s < j} q_s d_s + 0 + \sum_{j' > j} \frac{1}{1 - p_{v_j}} q_{j'} d_{j'} \\ &= \sum_{s=1}^n q_s d_s - q_j d_j + \sum_{j' > j} \frac{p_{v_j}}{1 - p_{v_j}} q_{j'} d_{j'} \\ &= \tilde{f}_{\text{ms}}(p; i, h) - q_j d_j + \frac{p_{v_j}}{1 - p_{v_j}} \sum_{j' > j} q_{j'} d_{j'}. \end{aligned}$$

When $p' = \text{der}(v_j, 1; p)$, we have

$$\begin{aligned} \tilde{f}_{\text{ms}}(p'; i, h) &= p'_{v_1} d_1 + (1 - p'_{v_1}) p'_{v_2} d_2 + \cdots + (\prod_{s=1}^{n-1} (1 - p'_{v_s})) p'_{v_n} d_n \\ &= \left(\sum_{s < j} \prod_{k=1}^{s-1} (1 - p_{v_k}) p_{v_s} d_s \right) + \prod_{k'=1}^{j-1} (1 - p_{v_{k'}}) d_j \\ &= \left(\sum_{s < j} \prod_{k=1}^{s-1} (1 - p_{v_k}) p_{v_s} d_s \right) + \sum_{j' \geq j} \prod_{k'=1}^{j'-1} (1 - p_{v_{k'}}) p_{v_{j'}} d_{j'} \\ &= \sum_{s < j} q_s d_s + \sum_{j' \geq j} q_{j'} d_{j'} \\ &= \sum_{s=1}^n q_s d_s + 0 + \sum_{j' > j} q_{j'} (d_j - d_{j'}) \\ &= \tilde{f}_{\text{ms}}(p; i, h) + \sum_{j' > j} q_{j'} (d_j - d_{j'}). \end{aligned}$$

□

Lemma 6. \hat{f}_{cv} is a TUB of $\mathbb{1}(X \notin \mathcal{C})$.

Proof. As mentioned in Rem. 2, since $\hat{f}_{\text{cv}} = \mathbb{1}(X \notin \mathcal{C})$, \hat{f}_{cv} is a tight upper bound of $\mathbb{1}(X \notin \mathcal{C})$. □

Lemma 7. For any $p \in [0, 1]^n$ and $i \in [n]$, $\Pr_{X \sim p}[\{v_X \in V_X : (v_X, i) \in E\} \neq \emptyset] = \prod_{v \in [n] : (v, i) \in E} (1 - p_v)$.

Proof. We decompose the event $\{v_X \in V_X : (v_X, i) \in E\} \neq \emptyset = \bigwedge_{v : (v, i) \in E} (v \notin V_X)$. Since the subevents $v \notin V_X$ are mutually independent,

$$\Pr_{X \sim p}[\{v_X \in V_X : (v_X, i) \in E\} \neq \emptyset] = \prod_{v \in [n] : (v, i) \in E} (1 - p_v).$$

□

Lemma 8 (IDs of \tilde{f}_{cv}). For any $p \in [0, 1]^n$ and $i \in [n]$, if $(i, j) \notin E$, then $\Delta \tilde{f}_{\text{cv}}(j, 0, p; i) = \Delta \tilde{f}_{\text{cv}}(j, 1, p; i) = 0$; if $(i, j) \in E$, then

$$\begin{cases} \Delta \tilde{f}_{\text{cv}}(j, 0, p; i) = p_j \prod_{v \in N_i, v \neq j} (p_v - 1), \\ \Delta \tilde{f}_{\text{cv}}(j, 1, p; i) = -\tilde{f}_{\text{cv}}(p; i). \end{cases}$$

Proof. If $(i, j) \notin E$, the value of p_j does not affect $\tilde{f}_{cv}(p; i)$ since p_j is not involved in the value of $\tilde{f}_{cv}(p; i)$. When $(i, j) \in E$, if $p' = \text{der}(j, 0; p)$,

$$\prod_{v \in N_i} (1 - p'_v) = \prod_{v \in N_i, v \neq j} (1 - p_v) = \tilde{f}_{cv}(p; i) - p_j \prod_{v \in N_i, v \neq j} (1 - p_v);$$

if $p' = \text{der}(j, 1; p)$,

$$\prod_{v \in N_i} (1 - p'_v) = 0.$$

□

Lemma 10. For any $p \in [0, 1]^n$, $\mathbb{E}_{X \sim p} \hat{f}_{cq}(X) = \sum_{(u,v) \in \binom{V}{2} \setminus E} p_u p_v$.

Proof. By linearity of expectation and double counting,

$$\hat{f}_{cq}(X) = \sum_{(u,v) \in \binom{V_X}{2}} \mathbb{1}[(u, v) \notin E] = \sum_{(u,v) \notin E} \mathbb{1}[(u, v) \in \binom{V_X}{2}].$$

Then we take the expectation and use the mutual independency among $v \in V_X$'s to get

$$\mathbb{E}_{X \sim p} [\hat{f}_{cq}(X)] = \sum_{(u,v) \notin E} \Pr[(u, v) \in \binom{V_X}{2}] = \sum_{(u,v) \notin E} p_u p_v.$$

□

Lemma 11 (IDs of \tilde{f}_{cq}). For any $p \in [0, 1]^n$ and $i \in [n]$,

$$\begin{cases} \Delta \tilde{f}_{cq}(i, 0, p) = -p_i \sum_{j \in [n], j \neq i, (i,j) \notin E} p_j, \\ \Delta \tilde{f}_{cq}(i, 1, p) = (1 - p_i) \sum_{j \in [n], j \neq i, (i,j) \notin E} p_j. \end{cases}$$

Proof. When $p' = \text{der}(i, 0; p)$,

$$\tilde{f}_{cq}(p') = \sum_{(u,v) \in \binom{V}{2} \setminus E} p'_u p'_v = \sum_{(u,v) \in \binom{V}{2} \setminus E, u \neq i, v \neq i} p_u p_v = \tilde{f}_{cq}(p) - p_i \sum_{j \in [n], j \neq i, (i,j) \notin E} p_j.$$

When $p' = \text{der}(i, 1; p)$,

$$\tilde{f}_{cq}(p') = \sum_{(u,v) \in \binom{V}{2} \setminus E, u \neq i, v \neq i} p_u p_v + \sum_{(i,j) \in \binom{V}{2} \setminus E} p_j = \tilde{f}_{cq}(p) + (1 - p_i) \sum_{j \in [n], j \neq i, (i,j) \notin E} p_j.$$

□

Lemma 12. \hat{g}_1 is a TUB of g_1 and \hat{f}_2 is a TUB of f_2 .

Proof. When $X \notin \mathcal{C}_1$, at least one edge in E_h is violated, i.e., $\hat{g}_1(X) \geq 1$. When $X \in \mathcal{C}_1$, no edge in E_h is violated, i.e., $\hat{g}_1(X) = 0$.

$\hat{f}_2 = f_2$ is a TUB of itself.

□

Lemma 13. For any $p \in [0, 1]^{n \times c}$, $\tilde{f}_2(p) = \mathbb{E}_{X \sim p} \hat{f}_2(X) = -\sum_{e=(u,v) \in E_s} \sum_{r=0}^{c-1} p_{ur} p_{vr} \log(1 - P(e))$ and $\tilde{g}_1(p) = \mathbb{E}_{X \sim p} \hat{g}_1(X) = \sum_{(u,v) \in E_h} \sum_{r=0}^{c-1} p_{ur} p_{vr}$.

Proof. We have

$$\begin{aligned}
 \mathbb{E}_{X \sim p} \hat{f}_2(X) &= \mathbb{E}_{X \sim p} - \sum_{e=(u,v) \in E_s: X_u = X_v} \log(1 - P(e)) \\
 &= \mathbb{E}_{X \sim p} - \sum_{e=(u,v) \in E_s} \mathbb{1}(X_u = X_v) \log(1 - P(e)) \\
 &= - \sum_{e=(u,v) \in E_s} \Pr_{X \sim p}[X_u = X_v] \log(1 - P(e)) \\
 &= - \sum_{e=(u,v) \in E_s} \sum_{r=0}^{c-1} \Pr_{X \sim p}[\text{both } u \text{ and } v \text{ have color } r] \log(1 - P(e)) \\
 &= - \sum_{e=(u,v) \in E_s} \sum_{r=0}^{c-1} p_{ur} p_{vr} \log(1 - P(e))
 \end{aligned}$$

and

$$\begin{aligned}
 \mathbb{E}_{X \sim p} \hat{g}_1(X) &= \mathbb{E}_{X \sim p} |\{(u, v) \in E_h: X_u = X_v\}| \\
 &= \mathbb{E}_{X \sim p} \sum_{(u,v) \in E_h} \mathbb{1}(X_u = X_v) \\
 &= \sum_{(u,v) \in E_h} \Pr_{X \sim p}[X_u = X_v] \\
 &= \sum_{(u,v) \in E_h} \Pr_{X \sim p}[\text{both } u \text{ and } v \text{ have color } r] \\
 &= \sum_{(u,v) \in E_h} \sum_{r=0}^{c-1} p_{ur} p_{vr}.
 \end{aligned}$$

□

Lemma 14 (IDs of the terms in \tilde{f}_{RC}). *For any $p \in [0, 1]^{n \times c}$, $i \in [n]$, and $x \in d$, $\Delta \tilde{g}_1(i, x; p) = \sum_{x' \in d \setminus \{x\}} p_{ix'} \sum_{(i,j) \in E_h} (p_{jx} - p_{jx'})$ and $\Delta \tilde{f}_2(i, x; p) = \sum_{x' \in d \setminus \{x\}} p_{ix'} \sum_{(i,j) \in E_s} (p_{jx'} - p_{jx}) \log(1 - P(i, j))$.*

Proof. When $p' = \text{der}(i, x; p)$,

$$\begin{aligned}
 \tilde{g}_1(\text{der}(i, x; p)) &= \sum_{(u,v) \in E_h} \sum_{r=0}^{c-1} p'_{ur} p'_{vr} \\
 &= \sum_{(u,v) \in E_h} \sum_{r=0}^{c-1} p'_{ur} p'_{vr} \\
 &= \sum_{(u,v) \in E_h, u \neq i, v \neq i} \sum_{r=0}^{c-1} p_{ur} p_{vr} + \sum_{(i,j) \in E_h} p_{jx} \\
 &= \tilde{g}_1(p) + (1 - p_{ix}) \sum_{(i,j) \in E_h} p_{jx} - \sum_{x' \in d \setminus \{x\}} p_{ix'} \sum_{(i,j) \in E_h} p_{jx'} \\
 &= \tilde{g}_1(p) + \sum_{x' \in d \setminus \{x\}} p_{ix'} \sum_{(i,j) \in E_h} (p_{jx} - p_{jx'}),
 \end{aligned}$$

where $1 - p_{ix} = \sum_{x' \in d \setminus \{x\}} p_{ix'}$ has been used. Similarly,

$$\begin{aligned}
 \tilde{f}_2(\text{der}(i, x; p)) &= - \sum_{e=(u,v) \in E_s} \sum_r p'_{ur} p'_{vr} \log(1 - P(e)) \\
 &= - \sum_{e=(u,v) \in E_s, u \neq i, v \neq i} \sum_r p'_{ur} p'_{vr} \log(1 - P(e)) - \sum_{e=(i,j) \in E_s} p_{jx} \log(1 - P(e)) \\
 &= \tilde{f}_2(p) - (1 - p_{ix}) \sum_{(i,j) \in E_s} p_{jx} \log(1 - P(i, j)) + \sum_{x' \in d \setminus \{x\}} p_{ix'} \sum_{(i,j) \in E_s} p_{jx'} \log(1 - P(i, j)) \\
 &= \tilde{f}_2(p) + \sum_{x' \in d \setminus \{x\}} p_{ix'} \sum_{(i,j) \in E_s} (p_{jx'} - p_{jx}) \log(1 - P(i, j)).
 \end{aligned}$$

□

B. Additional Details on the Background

We would like to provide some additional details on the background (Section 2.2).

B.1. On the “Differentiable Optimization” in the Pipeline (Section 2.2.1)

One can directly optimize a probabilistic decision p on each test instance G_{test} , i.e., aim to find $p^* \approx \arg \min_p \tilde{f}(p; G_{\text{test}})$. One can also train an encoder (e.g., a graph neural network) parameterized by parameters θ on a training set $\mathcal{D}_{\text{train}}$ to learn to output “good” (probabilistic) decisions for each training instance, i.e., aim to find $\theta^* \approx \arg \min_{\theta} \sum_{G \in \mathcal{D}_{\text{train}}} \tilde{f}(\text{ENCODER}(G; \theta); G)$. Such a trained encoder can be applied to each test instance G_{test} and output a (probabilistic) decision $p = \text{ENCODER}(G_{\text{test}}; \theta)$. Training such an encoder is optional, but if trained well, it can save time for unseen cases since we do not need to optimize p for each test instance from scratch.¹⁴ Even when using such an encoder, one can still further directly optimize the probabilistic decisions on each test instance. See more discussions on inductive settings and transductive settings in Appendix H.1.

B.2. Formal Theoretical Results in the Existing Works

Here, we would like to provide the detailed formal theoretical results in the existing works by Karalias & Loukas (2020) and Wang et al. (2022). Recall that Karalias & Loukas (2020) showed a quality guarantee by *random sampling*.

Theorem 3 (Theorem 1 by Karalias & Loukas (2020)). *Assume that f is non-negative.¹⁵ Fix any $\beta > \max_{X \in \mathcal{C}} f(X; G)$, $\epsilon > 0$, and $t \in (0, 1]$ such that $(1 - t)\epsilon < \beta$. For each $p \in [0, 1]^n$, if $\tilde{f}(p; G) < \beta$, then $\Pr_{X \sim p}[f(X; G) < \epsilon \wedge X \in \mathcal{C}] \geq t$.*

Recall that Wang et al. (2022) further proposed *iterative rounding*. Also, recall the following definitions: given a probability decision $p \in [0, 1]^n$, an index $i \in [n]$, and $x \in \{0, 1\}$, let $\text{der}(i, x; p)$ denoted the result after the i -th entry of p being *locally derandomized* as x . Formally, $\text{der}(i, x; p)_i = x$, and $\text{der}(i, x; p)_j = p_j, \forall j \neq i$. A probabilistic objective f is *entry-wise concave* if $p_i \tilde{f}(\text{der}(i, 1; p); G) + (1 - p_i) \tilde{f}(\text{der}(i, 0; p); G) \leq \tilde{f}(p; G), \forall G, p, i$.

Theorem 4 (Theorem 1 by Wang et al. (2022)). *If $\tilde{f}(p) \geq \mathbb{E}_{X \sim p} f(X) + \beta \Pr_{X \sim p}[X \notin \mathcal{C}], \forall p$ and \tilde{f} is entry-wise concave and non-negative with $\beta > \max(\tilde{f}(p_{\text{init}}), \max_{X \in \mathcal{C}} f(X))$, then for any permutation $\pi : [n] \rightarrow [n]$, starting from $p_{\text{cur}} = p_{\text{init}}$ and for $i \in [n]$ doing (1) $x^* \leftarrow \arg \min_{x \in \{0, 1\}} \tilde{f}(\text{der}(\pi(i), x; p_{\text{cur}}))$ and (2) $p_{\text{cur}} \leftarrow \text{der}(i, x^*; p_{\text{cur}})$ will finally give a discrete $p_{\text{final}} \in \mathcal{C}$ such that $f(p_{\text{final}}) < \tilde{f}(p_{\text{init}})$.*

B.3. Complex Conditions in Existing Works

As mentioned in Section 4, several conditions have been encountered in existing works. Here, for each condition analyzed in Section 4, we shall discuss how the existing works try to handle it.

Cardinality constraints. Wang et al. (2023) specifically considered cardinality constraints. However, they used optimal transport soft top- k instead of the probabilistic-method UL4CO we focus on in this work. Also, our derivation is more general since it can handle general cardinality constraints other than choosing a specific number of entities (i.e., top- k). Wang et al. (2023) claimed that cardinality constraints cannot be handled in the EGN pipeline, but this work shows that cardinality constraints can actually be properly handled by our derivations.

Minimum (maximum) w.r.t. a subset. Wang et al. (2023) also encountered such a condition in the facility location problem which they considered. They used the softmin to approximate the min operation, which indeed provides an upper bound. However, the result of softmin is not entry-wise concave, and thus fails to satisfy the good property required by Wang et al. (2022), while our derivation satisfies all the good properties.

Covering. Wang et al. (2023) also encountered such a condition in the maximum coverage problem which they considered. They used $\min(1, \sum_{v \in N_i} p_v)$ as an approximation for the probability of i being covered, where $N_i = \{v : (v, i) \in E\}$. In other words, they used $\max(0, 1 - \sum_{v \in N_i} p_v)$ to approximate the probability that i is not covered. As we have shown, the probability that i is not covered is exactly $\prod_{v \in N_i} (1 - p_v)$. However, $\max(0, 1 - \sum_{v \in N_i} p_v)$ is not an *upper bound* of $\prod_{v \in N_i} (1 - p_v)$ but a *lower bound*. Therefore, the derivation by Wang et al. (2023) does not satisfy the conditions required for the probabilistic-method UL4CO pipeline and thus does not satisfy the good properties.

¹⁴See some related discussions at https://github.com/Stalence/erdos_neu.

¹⁵We can always ensure this for any bounded f by adding a sufficiently large positive constant to f .

Cliques (or independent sets). Karalias & Loukas (2020) also considered the maximum clique problem, while our high-level targets provide insights into interpreting the derivation. Our derivation of incremental differences is novel, and we also showed how we can extend this to non-binary cases.

Other problems. Recently, UL4CO on the traveling salesman problem (TSP) has also been considered (Min et al., 2023), but their derivation does not satisfy the conditions required for the probabilistic-method UL4CO pipeline (see Section 2.2.1). We see the potential application of probabilistic-method UL4CO on TSP by seeing the conditions in TSP as a combination of (1) non-binary decisions and (2) cardinality constraints, both of which are already covered in this work. Specifically, if we aim to put n nodes in a cycle as the solution, then this can be understood as (1) deciding a position $X_v \in \{0, 1, \dots, n-1\}$ for each node $v \in [n]$ such that (2) each position contains exactly one node. See similar ideas in the (integer) linear programming formulations of TSP (Diaby, 2006; Yannakakis, 1988).

C. Additional Related Work

In the main text, we introduce the background with the most related works (Section 2.2). Here, we provide a more extensive literature review.

Unsupervised learning for combinatorial optimization. Most related are the works on unsupervised learning for combinatorial optimization (UL4CO). Karalias & Loukas (2020) first explicitly applied the probabilistic method to combinatorial optimization (CO) problems. UL4CO has been further explored and improved. Wang et al. (2022) formalized the rounding technique for derandomization and proposed some theoretically desirable properties for probabilistic objective formulation. Wang et al. (2023) focused on cardinality constraints, and instead of using the probabilistic method, they proposed a differentiable optimal-transport soft top- k method to handle cardinality constraints; see also Appendix B.3. We also see the potential future direction of extending UL4CO assuming dependence between decisions instead of assuming the decisions on the node are independent (Sanokowski et al., 2023), or using other distributions on the probabilistic decisions (Karalias et al., 2022). See Section 2.2 and Appendix B for more details.

Reinforcement learning for combinatorial optimization. There are also other learning-based methods proposed for CO problems. Typical techniques include reinforcement learning (RL). The pioneers who applied RL to CO problems include Bello et al. (2016) and Khalil et al. (2017). Most reinforcement-learning-for-combinatorial-optimization (RL4CO) methods focus on routing problems such as the traveling salesman problem (TSP) and the vehicle routing problem (VRP) (Berto et al., 2023; Kool et al., 2019; Kim et al., 2021; Delarue et al., 2020; Kim et al., 2022; Nazari et al., 2018; Ye et al., 2023a; Chalumeau et al., 2023; Luo et al., 2023; Grinsztajn et al., 2023), as well as maximum independent sets (MIP) (Ahn et al., 2020; Qiu et al., 2022; Sun & Yiming, 2023; Li et al., 2023). See also some recent surveys on RL4CO (Mazyavkina et al., 2021; Bengio et al., 2021; Cappart et al., 2023; Munikoti et al., 2023) for more details.

As pointed out by Wang et al. (2023) and as shown in our experimental results, the existing RL-based methods still suffer from efficiency issues. See the discussions by Wang et al. (2022). See also Appendix H.2 for some discussions on RL and probabilistic-method-based UL4CO. We also see the potential that probabilistic-method-based objective construction can also be used for reward design in RL methods.

Other machine-learning techniques for combinatorial optimization. Except for RL, there are also some other machine-learning techniques proposed for CO problems. We have recent progress based on search (Choo et al., 2022; Son et al., 2023; Li et al., 2023), sampling (Sun et al., 2023), graph-based diffusion (Sun & Yiming, 2023), generative flow networks (Zhang et al., 2023), meta-learning (Qiu et al., 2022; Wang & Li, 2023), and quantum machine learning (Ye et al., 2023b). Physics-inspired machine learning has also been considered (Schuetz et al., 2022a; Aramon et al., 2019; Schuetz et al., 2022b). There is also a line of research on perturbation-based methods for CO (Pogancic et al., 2019; Berthet et al., 2020; Paulus et al., 2021; Ferber et al., 2023). As shown by Wang et al. (2023), perturbation-based methods are consistently outperformed by CardNN proposed by Wang et al. (2023), while our proposed method outperforms CardNN in most cases.

D. Additional technical details

Here, we provide some additional technical details that are omitted in the main text.

D.1. Computation of the Poisson Binomial Distribution

Here, we provide some implementation details on the computation of the Poisson binomial distribution, which is used in Section 4.1. We mainly follow the original paper (Hong, 2013) and an existing implementation online (Straka, 2017).

The main formula is

$$\Pr_{X \sim p}[|V_X| = t] = \frac{1}{n+1} \sum_{s=0}^n \exp(-i\omega st) \prod_{j=1}^n (1 - p_j + p_j \exp(i\omega s)),$$

where $i = \sqrt{-1}$ and $\omega = \frac{2\pi}{n+1}$. See the original paper (Hong, 2013) for more technical details.

E. Additional Theoretical Results

Here, we provide additional theoretical results.

E.1. Additional Results on Non-Binary Decisions

Here, we provide the details of our theoretical results regarding non-binary decisions.

Notations. With non-binary decisions $d = \{0, 1, \dots, c-1\}$, we use $p \in [0, 1]^{n \times c}$ with $\sum_{r=0}^{c-1} p_{ir} = 1, \forall i \in [n]$ to represent the probabilities of possible decisions, where each $p_{ir} = \Pr[X_i = r]$. Now, $\text{der}(i, x; p)$ is the result after the i -th row of p being

$$\text{locally derandomized w.r.t. its } x\text{-th entry, i.e., } \begin{cases} \text{der}(i, x; p)_{ix} = 1, \\ \text{der}(i, y; p)_{iy} = 0, \forall y \neq x, \text{ and} \\ \text{der}(i, x; p)_{jz} = p_{jz}, \forall j \neq i, \forall z. \end{cases}$$

Theoretical analysis on non-binary cases. Our theoretical results (Thms. 1 & 2) can be extended to non-binary cases.¹⁶ With non-binary decisions, a probabilistic objective $\tilde{f} : [0, 1]^{n \times c} \rightarrow \mathbb{R}$ is *entry-wise concave* if

$$\sum_{r \in d} p_{ir} \tilde{f}(\text{der}(i, r; p)) \leq \tilde{f}(p), \forall p \in [0, 1]^{n \times c}, i \in [n],$$

and the process of greedy derandomization is:

$$\begin{cases} (1) (i^*, x^*) \leftarrow \arg \min_{(i, x) \in [n] \times d} \tilde{f}(\text{der}(i, x; p_{\text{cur}})) \text{ and} \\ (2) p_{\text{cur}} \leftarrow \text{der}(i^*, x^*; p_{\text{cur}}). \end{cases}$$

Theorem 5 (Expectations are all you need (non-binary version)). *For any function $g : d^n \rightarrow \mathbb{R}$, $\tilde{g} : [0, 1]^{n \times c} \rightarrow \mathbb{R}$ with $\tilde{g}(p) = \mathbb{E}_{X \sim p} g(X)$ is differentiable and entry-wise concave, where $\mathbb{E}_{X \sim p} g(X) = \sum_{X \in d^n} \Pr_p[X] g(X)$ with $\Pr_p[X] = \prod_{v \in [n]} p_{vX_v}$.*

¹⁶See App. E.1 for the detailed statements, where we also extend the theoretical results in the existing works by Karalias & Loukas (2020) and Wang et al. (2022) to non-binary cases.

Proof. For any p and i , we have

$$\begin{aligned}
 \tilde{g}(p) &= \mathbb{E}_{X \sim p} g(X) \\
 &= \sum_{X \in d^n} \Pr[X] g(X) \\
 &= \sum_{X \in d^n} \prod_{v \in [n]} p_{vX_v} g(X) \\
 &= \sum_{X \in d^n} \left(\prod_{v \in [n] \setminus \{i\}} p_{vX_v} \right) p_{iX_i} g(X) \\
 &= \sum_{r \in d} \sum_{X: X_i=r} \left(\prod_{v \in [n] \setminus \{i\}} p_{vX_v} \right) p_{iX_i} g(X) \\
 &= \sum_{r \in d} \sum_{X: X_i=r} \left(\prod_{v \in [n] \setminus \{i\}} p_{vX_v} \right) p_{ir} g(X) \\
 &= \sum_{r \in d} p_{ir} \sum_{X: X_i=r} \left(\prod_{v \in [n] \setminus \{i\}} p_{vX_v} \right) g(X) \\
 &= \sum_{r \in d} p_{ir} \sum_X \left(\prod_{v \in [n] \setminus \{i\}} p_{vX_v} \right) \mathbb{1}(X_i = r) g(X) \\
 &= \sum_{r \in d} p_{ir} \tilde{g}(\text{der}(i, r; p)) \\
 &\geq \sum_{r \in d} p_{ir} \tilde{g}(\text{der}(i, r; p)),
 \end{aligned}$$

completing the proof on entry-wise concavity. Regarding differentiability, since $\mathbb{E}_{X \sim p} g(X) = \sum_{X \in d^n} \Pr_p[X] g(X)$, it suffices to show that $\Pr_p[X] g(X) = \sum_{X \in d^n} \prod_{v \in [n]} p_{vX_v} g(X)$ is differentiable w.r.t p for each $X \in \{0, 1\}^n$. Indeed, fix any X , $\sum_{X \in d^n} \prod_{v \in [n]} p_{vX_v} g(X)$ is a polynomial of p_{ir} 's, and is thus differentiable. \square

With non-binary decisions, the process of greedy derandomization is extended as follows:

- (1) $(i^*, x^*) \leftarrow \arg \min_{(i, x) \in [n] \times d} \tilde{f}(\text{der}(i, x; p_{\text{cur}}))$ and
- (2) $p_{\text{cur}} \leftarrow \text{der}(i^*, x^*; p_{\text{cur}})$.

Theorem 6 (Goodness of greedy derandomization (non-binary version)). *Theorem 2 still holds in non-binary cases, i.e., with $\{0, 1\}$ being replaced by any non-binary d . Specifically, for any entry-wise concave \tilde{f} and p_{init} , the above process can always reach a point where the final p_{final} is (1) discrete (i.e., $p_{\text{final}} \in d^n$), (2) no-worse than p_{init} (i.e., $\tilde{f}(p_{\text{final}}) \leq \tilde{f}(p_{\text{init}})$), and (3) is a local minimum (i.e., $\tilde{f}(p_{\text{final}}) = \min_{(i, x) \in [n] \times d} \tilde{f}(\text{der}(\pi(i), x; p_{\text{final}}))$).*

Proof. See the proof for Theorem 2. It is easy to see that the reasoning still holds with $\{0, 1\}$ being replaced by any non-binary d . \square

We also extend the theoretical results in the existing works (Karalias & Loukas, 2020; Wang et al., 2022) to non-binary cases.

Recall the theoretical results (Theorem 3) by Karalias & Loukas (2020).

Theorem 3 (Theorem 1 by Karalias & Loukas (2020)) Assume that f is non-negative. Fix any $\beta > \max_{X \in \mathcal{C}} f(X; G)$, $\epsilon > 0$, and $t \in (0, 1]$ such that $(1 - t)\epsilon < \beta$. If $\tilde{f}(p_{\text{init}}; G) < \beta$, then $\Pr_{X \sim p_{\text{init}}} [f(X; G) < \epsilon \wedge X \in \mathcal{C}] \geq t$.

We extend Theorem 3 to non-binary cases.

Theorem 7 (Non-binary extension of Theorem 3). Assume that f is non-negative. Fix any $\beta > \max_{X \in \mathcal{C}} f(X; G)$, $\epsilon > 0$, and $t \in (0, 1]$ such that $(1 - t)\epsilon < \beta$. If $\tilde{f}(p_{\text{init}}; G) < \beta$, then $\Pr_{X \sim p_{\text{init}}} [f(X; G) < \epsilon \wedge X \in \mathcal{C}] \geq t$.

Proof. We shall follow the main idea in the original proof of Theorem 3 by Karalias & Loukas (2020), which is based on Markov's inequality. The key point is that the reasoning still holds when the decisions are non-binary. Specifically, we can define a probabilistic penalty function $\hat{f}(X; G) = f(X; G) + \beta \mathbb{1}(X \in \mathcal{C})$. Since $\beta > \max_{X \in \mathcal{C}} f(X; G)$, we have

$\hat{f}(X; G) < \epsilon$ if and only if $f(X; G) < \epsilon$ and $X \in \mathcal{C}$. Therefore, using Markov's inequality, we have

$$\begin{aligned} \Pr_{X \sim p_{\text{init}}} [(f(X; G) < \epsilon) \wedge (X \in \mathcal{C})] &= \Pr_{X \sim p_{\text{init}}} [\hat{f}(X; G) < \epsilon] \\ &> 1 - \frac{1}{\epsilon} \mathbb{E}_{X \sim p_{\text{init}}} [\hat{f}(X; G)] \\ &= 1 - \frac{1}{\epsilon} \mathbb{E}_{X \sim p_{\text{init}}} [f(X; G) + \beta \mathbb{1}(X \in \mathcal{C})] \\ &> 1 - \frac{1}{\epsilon} (\beta) \\ &> t. \end{aligned}$$

□

Recall the theoretical results (Theorem 4) by Wang et al. (2022).

Theorem 4 (Theorem 1 by Wang et al. (2022)) If $\tilde{f}(p) \geq \mathbb{E}_{X \sim p} f(X) + \beta \Pr_{X \sim p}[X \notin \mathcal{C}]$, $\forall p$ is entry-wise concave and non-negative with $\beta > \max(\tilde{f}(p_{\text{init}}), \max_{X \in \mathcal{C}} f(X))$, then for any permutation $\pi : [n] \rightarrow [n]$, starting from $p_{\text{cur}} = p_{\text{init}}$ and for $i \in [n]$ doing (1) $x^* \leftarrow \arg \min_{x \in \{0,1\}} \tilde{f}(\text{der}(\pi(i), x; p_{\text{cur}}))$ and (2) $p_{\text{cur}} \leftarrow \text{der}(i, x^*; p_{\text{cur}})$ will finally give a discrete $p_{\text{final}} \in \mathcal{C}$ such that $f(p_{\text{final}}) \leq \tilde{f}(p_{\text{init}})$.

We shall show that Theorem 4 can be extended to non-binary cases.

Theorem 8 (Non-binary extension of Theorem 4). If $\tilde{f}(p) \geq \mathbb{E}_{X \sim p} f(X) + \beta \Pr_{X \sim p}[X \notin \mathcal{C}]$, $\forall p$ is entry-wise concave and non-negative with $\beta > \max(\tilde{f}(p_{\text{init}}), \max_{X \in \mathcal{C}} f(X))$, then for any permutation $\pi : [n] \rightarrow [n]$, starting from $p_{\text{cur}} = p_{\text{init}}$ and for $i \in [n]$ doing (1) $x^* \leftarrow \arg \min_{x \in \{0,1,2,\dots,c-1\}} \tilde{f}(\text{der}(\pi(i), x; p_{\text{cur}}))$ and (2) $p_{\text{cur}} \leftarrow \text{der}(i, x^*; p_{\text{cur}})$ will finally give a discrete $p_{\text{final}} \in \mathcal{C}$ such that $f(p_{\text{final}}) \leq \tilde{f}(p_{\text{init}})$.

Proof. We shall follow the main idea in the original proof of Theorem 4 by Wang et al. (2022), where the key idea was that entry-wise concavity ensures that local derandomization does not increase the objective. This key idea still holds with non-binary decisions. First, since after the series of local derandomization, for each i , it is locally derandomized exactly once, the final derandomized result should be discrete. Regarding $p_{\text{final}} \in \mathcal{C}$ and $f(p_{\text{final}}) \leq \tilde{f}(p_{\text{init}})$, we claim that “local derandomization does not increase the objective”. Specifically, since \tilde{f} is entry-wise concave, i.e.,

$$\sum_{r \in d} p_{ir} \tilde{f}(\text{der}(i, r; p); G) \leq \tilde{f}(p; G), \forall G, p, i,$$

and $\sum_{r \in d} p_{ir} = 1$, we have

$$\min_{r \in d} \tilde{f}(\text{der}(i, r; p); G) \leq \sum_{r \in d} p_{ir} \tilde{f}(\text{der}(i, r; p); G) \leq \tilde{f}(p; G), \forall G, p, i.$$

Hence, indeed, “local derandomization does not increase the objective”, and the final

$$f(X; G) + \beta \mathbb{1}(X \notin \mathcal{C}) \leq \tilde{f}(p_{\text{init}}) < \beta,$$

which implies that $f(X; G) \leq \tilde{f}(p_{\text{init}})$ and $\mathbb{1}(X \notin \mathcal{C}) = 0$, i.e., $X \in \mathcal{C}$, completing the proof. □

F. Additional Problems

The robust k -clique problem generalizes the maximum k -clique problem (Bomze et al., 1999) and it can be seen as an uncertain variant of the heaviest k -subgraph problem (Feige et al., 2001; Billonnet, 2005).

F.1. Robust k -Clique

Definition. Given (1) an uncertain graph $G = (V, E, P)$, and (2) $k \in \mathbb{N}$, we aim to find a subset of nodes $V_X \subseteq V$ such that (c1) $|V_X| = k$, (c2) V_X forms a clique, and (c3) $\Pr[\text{all the edges between nodes in } V_X \text{ exist}]$ is maximized.

Involved conditions: (1) cardinality constraints, (2) cliques, and (3) uncertainty (see Sections 4.1, 4.4 & 4.6).

Details. Regarding conditions (c1)-(c2), we can directly use the derivations for them. Regarding condition (c3), fix any V_X , the probability that all the edges between nodes in V_X exist is

$$\prod_{(u,v) \in \binom{V_X}{2} \cap E} P_{uv}.$$

Maximizing the probability is equivalent to minimizing

$$f_1(X) := - \sum_{(u,v) \in \binom{V_X}{2} \cap E} \log P_{uv}.$$

We let $\hat{f}_1(X) := f_1(X)$ and let

$$\tilde{f}_1(p) := \mathbb{E}_{X \sim p} \hat{f}_1(X) = - \sum_{(u,v) \in E} p_u p_v \log P_{uv}.$$

The final objective is

$$\tilde{f}_{\text{RQ}}(p) = \tilde{f}_1(p) + \beta_1 \tilde{f}_{\text{cq}}(p) + \beta_2 \tilde{f}_{\text{card}}(p; \{k\})$$

with constraint coefficients $\beta_1, \beta_2 > 0$.

Regarding the incremental differences, we only need to derive the incremental differences of \tilde{f}_1 , which is

$$\Delta \tilde{f}_1(i, 1, p) = (p_i - 1) \sum_{v: (i,v) \in E} p_v \log P_{iv},$$

and

$$\Delta \tilde{f}_1(i, 0, p) = -p_i \sum_{v: (i,v) \in E} p_v \log P_{iv}.$$

F.2. Robust Dominating Set

The robust dominating set problem generalizes the minimal dominating set problem [Guha & Khuller \(1998\)](#) and can also be seen as an uncertain version of set covering [Caprara et al. \(2000\)](#).

Definition. Given (1) an uncertain graph $G = (V, E, P)$, and (2) $k \in \mathbb{N}$, we aim to find a subset of nodes $V_X \subseteq V$ such that (c1) $|V_X| = k$, (c2) V_X is a dominating set in the underlying deterministic graph, that is, for each $v \in V$, either $v \in V_X$ or v has a neighbor in V_X , and (c3) the probability that V_X is indeed a dominating set when considering the edge uncertainty, i.e. $\Pr[\bigwedge_{v \in V \setminus V_X} \bigvee_{u \in V_X} A_{uv}]$ is maximized. For each edge $(u, v) \in E$, A_{uv} is the event that (u, v) exists under edge certainty, which happens with probability P_{uv} .

Involved conditions: (1) cardinality constraints, (2) covering, and (3) uncertainty (see Sections 4.1, 4.3, & 4.6).

Details. Regarding conditions (c1), we can directly use the derivations for it. Specifically, $\tilde{f}_1(p) = \tilde{f}_{\text{card}}(p; \{k\})$.

Conditions (c2) and (c3) can be combined together. We first add self-loops on each node $v \in V$ (so that each node v can cover v itself), and then consider the condition as $X \in \mathcal{C}$ with

$$\mathcal{C} = \{X : \text{each node } v \in V \text{ is covered}\}.$$

Then we define $\hat{f}_2(X)$ as the expected number of nodes that are not covered (when taking the edge uncertainty into consideration). It is easy to see that $\hat{f}_2(X) \geq \mathbb{1}(X \notin \mathcal{C})$, $\forall X \in \{0, 1\}^n$. Note that here the uncertainty comes from the edge probabilities while the decisions are discrete. The formula of \hat{f}_2 is

$$\hat{f}_2(X) = \sum_{i \in V} \Pr[i \text{ is not covered}] = \sum_{i \in V \setminus V_X} \prod_{v \in N_i} (1 - P_{iv}),$$

where $N_i = \{v \in V : (i, v) \in E\}$ is the neighborhood of i . We then define $\tilde{f}_2(p) = \mathbb{E}_{X \sim p} \hat{f}_2(X)$, and its formula is

$$\tilde{f}_2(p) = \sum_{i \in V} \Pr[i \notin V_X] \prod_{v \in N_i} (1 - P_{iv}) = \sum_{i \in V} (1 - p_i) \prod_{v \in N_i} (1 - P_{iv}).$$

Combining all the conditions, the final probabilistic objective is

$$\tilde{f}_{\text{RDS}}(p) = \tilde{f}_2(p) + \beta \tilde{f}_1(p)$$

with constraint coefficient $\beta > 0$.

Regarding the incremental differences, we only need to derive the incremental differences of \tilde{f}_2 , which is

$$\Delta \tilde{f}_2(i, 1, p) = (p_i - 1) \prod_{v \in N_i} (1 - P_{iv})$$

and

$$\Delta \tilde{f}_2(i, 0, p) = -p_i \prod_{v \in N_i} (1 - P_{iv}).$$

F.3. Clique Cover

The clique cover problem (Gramm et al., 2009) is a classical NP-hard combinatorial problem. We consider its decision version, which is NP-complete.

Definition. Given (1) a graph $G = (V, E)$ and (2) $c \in \mathbb{N}$, we aim to partition the nodes into c groups, such that each group forms a clique.

Involved conditions: (1) cliques and (2) non-binary decisions (see Sections 4.4 & 4.5).

Details. This is basically the non-binary extension of the “cliques” condition. For each $r \in d = \{0, 1, 2, \dots, c-1\}$, the condition holds for group- r if the group is either empty or forms a clique. The group- r is empty with probability $\prod_{i \in V} (1 - p_{ir})$, and we can use

$$\tilde{f}_{\text{cq}}(p_{\cdot, r}) \geq \Pr_{X \sim p}[\text{group-}r \text{ does not form a clique}],$$

where $p_{\cdot, r} \in [0, 1]^n$ with $(p_{\cdot, r})_j = p_{j, r}$. Then the violation probability

$$\begin{aligned} \Pr[\text{violation}] &= \Pr[\text{not empty} \wedge \text{does not form a clique}] \\ &\leq \Pr[\text{not empty}] + \Pr[\text{does not form a clique}]. \end{aligned}$$

Therefore, we can have the final probabilistic objective

$$\tilde{f}_{\text{cc}}(p) = \sum_{r=0}^{c-1} 1 - \prod_{i \in V} (1 - p_{ir}) + \tilde{f}_{\text{cq}}(p_{\cdot, r}).$$

If we create a complete graph K_V with self-loops on V , then

$$\prod_{i \in V} (1 - p_{ir}) = \tilde{f}_{\text{cv}}(p_{\cdot, r}; v, K_V)$$

for any $v \in V$. Hence, we have

$$\tilde{f}_{\text{CC}}(p) = \sum_{r=0}^{c-1} 1 - \tilde{f}_{\text{cv}}(p_{\cdot, r}; v, K_V) + \tilde{f}_{\text{cq}}(p_{\cdot, r}),$$

and the incremental differences can be handled by those of \tilde{f}_{cv} and \tilde{f}_{cq} .

F.4. Minimum Spanning Tree

The minimum spanning tree problem (Graham & Hell, 1985) is a classical combinatorial problem. Notably, it is not theoretically difficult and we have fast algorithms (Pettie & Ramachandran, 2002; Zhong et al., 2015) for the problem. But it is still interesting to see that our method can be applied to such a problem.

Definition. Given a graph $G = (V, E, W)$, we aim to find a subset of edges to form a connected tree (i.e., without cycles) containing all the nodes such that the total edge weights in the tree are minimized. Instead of considering choosing edges, we consider the decisions on nodes. Specifically, we put the nodes into different layers. Let $c \leq n$ be the number of layers,

it is a non-binary problem, where each node v is put into layer- X_v with $X_v \in d = \{0, 1, 2, \dots, c-1\}$. For each node v_ℓ in layer $\ell > 0$, it would be connected to a parent v_{prev} in the previous layer- $(\ell-1)$ so that the edge weight of (v_ℓ, v_{prev}) is minimized. The conditions are: (c1) each node is either in layer-0, or it can find a parent in the previous layer, and (c2) the total edge weights are minimized.

Involved conditions: (1) minimum (maximum) w.r.t. a subset, (2) covering and (3) non-binary decisions (see Sections 4.2, 4.3, and 4.5).

Details. Regarding (c1), we let \hat{f}_1 be the number of nodes for which (c1) is violated. For each node i , it is in layer-0 with probability p_{v0} and it can find at least one parent with probability

$$\begin{aligned} \sum_{\ell=1}^{c-1} \Pr[i \text{ is in layer-}\ell] \Pr[\text{at least one of } i\text{'s neighbors is in layer-}(\ell-1)] &= \sum_{\ell=1}^{c-1} p_{i\ell} \left(1 - \prod_{v \in N_i} (1 - p_{v, \ell-1})\right) \\ &= \sum_{\ell=1}^{c-1} p_{i\ell} (1 - \tilde{f}_{cv}(p, \ell-1; i)), \end{aligned}$$

where $p_{\cdot, \ell-1} \in [0, 1]^n$ with $(p_{\cdot, \ell-1})_j = p_{j, \ell-1}$. Again, $N_i = \{v \in V : (i, v) \in E\}$ is the neighborhood of i . Note how the idea of “covering” is used here. Therefore, the probability that (c1) is violated for the node i is

$$1 - p_{i0} - \sum_{\ell=1}^{c-1} p_{i\ell} (1 - \tilde{f}_{cv}(p, \ell-1; i)).$$

Now we are ready to compute

$$\tilde{f}_1(p) = \mathbb{E}_{X \sim p} \hat{f}_1(X) = \sum_{i \in V} (1 - p_{i0} - \sum_{\ell=1}^{c-1} p_{i\ell} (1 - \tilde{f}_{cv}(p, \ell-1; i))).$$

Regarding (c2), we use the idea of “minimum (maximum) w.r.t. a subset”. For a spanning tree, the total edge weights are

$$\sum_{i \in V : i \text{ not the root}} W(i, \text{the parent of } i).$$

Note that in a minimum spanning tree, each non-root node should have a single parent. For each node i , the expected $W(i, \text{the parent of } i)$ is

$$\sum_{\ell=1}^{c-1} p_{i\ell} \tilde{f}_{ms}(p_{\cdot, \ell-1}; i, W),$$

where $p_{\cdot, \ell-1} \in [0, 1]^n$ with $(p_{\cdot, \ell-1})_j = p_{j, \ell-1}$. The idea of “minimum (maximum) w.r.t. a subset” has been used, where we consider the nodes being chosen into layer- $(\ell-1)$. Therefore, we have

$$\tilde{f}_2(p) = \sum_{i \in V} \sum_{\ell=1}^{c-1} p_{i\ell} \tilde{f}_{ms}(p_{\cdot, \ell-1}; i, W).$$

Combining the conditions, the final probabilistic objective is

$$\tilde{f}_{\text{MST}}(p) = \tilde{f}_2(p) + \beta \tilde{f}_1(p)$$

with constraint coefficient $\beta > 0$. The incremental differences can be handled by those of \tilde{f}_{cv} and \tilde{f}_{ms} .

F.5. On cycles and trees

Cycles. As discussed in Appendix B.3, CO problems involving cycles can be handled as follows. The conditions that nodes should form a cycle can be seen as a combination of (1) non-binary decisions and (2) cardinality constraints. Specifically, if we aim to put n nodes in a cycle, then this can be understood as (1) deciding a position $X_v \in \{0, 1, \dots, n-1\}$ for each node $v \in [n]$ such that (2) each position contains exactly one node.

Trees. In MST (and other CO problems involving trees), an implicit condition is *acyclicity* (Lachapelle et al., 2020). In our way of organizing nodes into sequences of layers, acyclicity is naturally satisfied. However, this might be tricky if we also need to decide how each node chooses its parent(s) and child(ren). For MST, this is deterministic in the sense that each non-root node should always choose the closest node in the above layer as its only parent, so that the total distance is minimized. In general, we may need additional decisions (parameters) for the choice of edges.

G. Complete Experimental Settings and Results

Here, we provide detailed experimental settings and some additional experimental results.

G.1. Detailed Experimental Settings

Here, we provide some details of the experimental settings.

G.1.1. HARDWARE

All the experiments are run on a machine with two Intel Xeon® Silver 4210R (10 cores, 20 threads) processors, a 256GB RAM, and RTX2080Ti (11GB) GPUs. For the methods using GPUs, a single GPU is used.

G.1.2. FACILITY LOCATION

Here, we provide more details about the settings of the experiments on the facility location problem. For the experiments on facility location and maximum coverage, we mainly follow the settings by Wang et al. (2023) and use their open-source implementation.¹⁷

Datasets. We consider both random synthetic graphs and real-world graphs:

- **Rand500:** We follow the way of generating random graphs by Wang et al. (2023). We generate 100 random graphs, where each graph contains 500 nodes. Each node v has a two-dimensional location (x_v, y_v) , where x_v and y_v are sampled in $[0, 1]$, independently, uniformly at random.
- **Rand800:** The rand800 graphs are generated in a similar way. The only difference is that each rand800 graph contains 800 nodes.
- **Starbucks:** The Starbucks datasets were used by Wang et al. (2023). We quote their descriptions as follows: “The datasets are built based on the project named Starbucks Location Worldwide 2021 version,¹⁸ which is scraped from the open-accessible Starbucks store locator webpage.¹⁹ We analyze and select 4 cities with more than 100 Starbucks stores, which are London (166 stores), New York City (260 stores), Shanghai (510 stores), and Seoul (569 stores). The locations considered are the real locations represented as latitude and longitude.”
- **MCD:** The MCD (McDonald’s) dataset is available online.²⁰ The dataset contains the locations of MCD branches in the United States. We divide the dataset into multiple sub-datasets by state, where each sub-dataset contains branches in the same state. We use the data from 8 states with the most ranches: CA (1248 branches), TX (1155 branches), FL (889 branches), NY (597 branches), PA (483 branches), IL (650 branches), OH (578 branches), and GA (442 branches).
- **Subway:** The Subway dataset is available online.²¹ Similar to the MCD dataset, it contains the locations of subway branches in the United States. We also divide the dataset into multiple sub-datasets by state, where each sub-dataset contains branches in the same state. We use the data from 8 states with the most ranches: CA (2590 branches), TX (21994 branches), FL (1490 branches), NY (1066 branches), PA (865 branches), IL (1110 branches), OH (1171 branches), and GA (852 branches).
- For the real-world datasets, we use min-max normalization to make sure that each coordinate of each node (location) is also in $[0, 1]$ as in the random graphs.

Inductive settings. We follow the settings by Wang et al. (2023). For random graphs, the model is trained and tested on random graphs from the same distribution, but the training set and the test set are disjoint. For real-world graphs, the model is trained on the *rand500* graphs.

Methods. We consider both traditional methods and machine-learning methods:

¹⁷<https://github.com/Thinklab-SJTU/One-Shot-Cardinality-NN-Solver>

¹⁸<https://www.kaggle.com/datasets/kukuroo3/starbucks-locations-worldwide-2021-version>

¹⁹<https://www.starbucks.com/store-locator>

²⁰<https://www.kaggle.com/datasets/mdmdata/mcdonalds-locations-united-states>

²¹<https://www.kaggle.com/datasets/thedevastator/subway-the-fastest-growing-franchise-in-the-world>

- **Random:** Among all the locations, k locations are picked uniformly at random; 240 seconds are given on each test graph.
- **Greedy:** deterministic greedy algorithms. We use the implementation of Wang et al. (2023).
- **Gurobi** (Gurobi Optimization, LLC, 2023) and **SCIP** (Bestuzheva et al., 2021; Perron & Furnon, 2023): The problems are formulated as MIPs and the two solvers are used; the time budget is set as 120 seconds, but the programs sometimes do not terminate until more time is used.
- **CardNN** (Wang et al., 2023): Three variants proposed in the original paper. We use the implementation of the original authors.
- **CardNN-noTTO:** In addition to training, CardNN also directly optimizes on each test graph in test time, and this is a variant of CardNN without test-time optimization. We use the implementation of the original authors.
- **EGN-naive:** EGN (Karalias & Loukas, 2020) with a naive objective construction and iterative rounding, which was used by Wang et al. (2023) as a baseline method. We use the derivation and implementation by Wang et al. (2023).
- **RL:** A reinforcement-learning method (Kool et al., 2019). We adapt the implementation by Berto et al. (2023).²²

Speed-quality trade-offs. For the proposed method UCOM2, we use test-time augmentation (Jin et al., 2023) on the test graphs by adding perturbations into both graph topology and features to obtain additional data. Specifically, we use edge dropout (Papp et al., 2021; Shu et al., 2022) and add Gaussian noise into features. The noise scale and the edge dropout ratios are both 0.2, which we do not fine-tune. The three variants of UCOM2 are obtained by using different numbers of additional augmented data and taking the best objective. Specifically, the “short” version uses only the original test graphs, the “middle” version uses less time than CardNN-GS, and the “long” version uses less time than CardNN-HGS.

Evaluation. Given locations (x_v, y_v) ’s for the nodes $v \in V$, if the final selected k nodes are v_1, v_2, \dots, v_k , the final objective is $\sum_{v \in V} \min_{i \in [k]} \text{dist}(v_i, v)$, where the distance metric dist is the Euclidean squared distance used by Wang et al. (2023). We choose $k = 30$ locations in each graph, except for the rand800 graphs where we choose $k = 50$ locations.

Hyperparameter fine-tuning. For the proposed method UCOM2 and the method CardNN by Wang et al. (2023), we conduct hyperparameter fine-tuning. For UCOM2, we fine-tune the learning rate (LR) and constraint coefficient (CC). For CardNN, we fine-tune the training learning rate (LR)²³ and the Gumbel noise scale σ . For random graphs, we choose the best hyperparameter setting w.r.t. the objective on the training set, because the distribution of the training set and the distribution of the test set are the same. For real-world graphs, we choose the smallest graph in each group of datasets as the validation graph, and we choose the best hyperparameter setting w.r.t. the objective on the validation graph. There is no specific reason to choose the smallest, and we just want to have a deterministic way to choose validation graphs.

We make sure that the number of candidate combinations (which is 15) is the same for both methods. Our hyperparameter search space is as follows:

- For UCOM2: $\text{LR} \in \{1e-1, 1e-2, 1e-3, 1e-4, 1e-5\}$ and $\text{CC} \in \{1e-1, 1e-2, 1e-3\}$
- For CardNN: $\text{LR} \in \{1e-1, 1e-2, 1e-3, 1e-4, 1e-5\}$ and $\sigma \in \{0.01, 0.15, 0.25\}$

Notably, after our fine-tuning, the performance of CardNN is at least the same and usually better than the performance using the hyperparameter settings in the open-source code of CardNN provided by the original authors. The best hyperparameter settings for each dataset are:

- Rand500:
 - UCOM2: $\text{LR} = 1e-1, \text{CC} = 1e-1$
 - CardNN: $\text{LR} = 1e-4, \sigma = 0.25$

- Rand800:

²²<https://github.com/kaist-silab/rl4co>

²³CardNN uses (possibly) different learning rates for training and test-time optimization.

– UCom2: LR = $1e-2$, CC = $1e-2$

– CardNN: LR = $1e-4$, $\sigma = 0.25$

• Starbucks:

– UCom2: LR = $1e-1$, CC = $1e-1$

– CardNN: LR = $1e-4$, $\sigma = 0.15$

• MCD:

– UCom2: LR = $1e-3$, CC = $1e-1$

– CardNN: LR = $1e-5$, $\sigma = 0.25$

• Subway:

– UCom2: LR = $1e-1$, CC = $1e-1$

– CardNN: LR = $1e-5$, $\sigma = 0.01$

G.1.3. MAXIMUM COVERAGE

Here, we provide more details about the settings of the experiments on the maximum coverage problem.

Datasets. We consider both random synthetic graphs and real-world graphs:

- **Rand500:** We follow the way of generating random graphs by Wang et al. (2023). Each item has a random weight chosen uniformly at random between 1 and 100. Each set contains a random number of items, and the number of items is chosen uniformly at random between 10 and 30. Each rand500 dataset contains 500 sets and 1000 items.
- **Rand1000:** The rand1000 graphs are generated in a similar way. The only difference is that each rand1000 dataset contains 1000 sets and 2000 items.
- **Twitch:** The Twitch datasets were used by Wang et al. (2023). We quote their descriptions as follows: “This social network dataset is collected by Rozemberczki et al. (2021) and the edges represent the mutual friendships between streamers. The streamers are categorized by their streaming language, resulting in 6 social networks for 6 languages. The social networks are DE (9498 nodes), ENGB (7126 nodes), ES (4648 nodes), FR (6549 nodes), PTBR (1912 nodes), and RU (4385 nodes). The objective is to cover more viewers, measured by the sum of the logarithmic number of viewers. We took the logarithm to enforce diversity because those top streamers usually have the dominant number of viewers.”
- **Railway:** The railway datasets (Ceria et al., 1998) are available online.²⁴ The data were collected from real-world crew membership in Italian railways. We have three datasets: (1) rail507 with 507 sets and 63009 items, (2) rail516 with 516 sets and 47311 items, and (3) rail582 with 582 sets and 55515 items.

Inductive settings. We follow the settings by Wang et al. (2023). For random graphs, the model is trained and tested on random graphs from the same distribution, but the training set and the test set are disjoint. For real-world graphs, the model is trained on the *rand500* graphs.

Methods. See the method descriptions above for the facility location problem in Appendix G.1.2.

Speed-quality trade-offs. See the descriptions above for the facility location problem in Appendix G.1.2.

Evaluation. Let w_j ’s denote the weights of the items. The final objective is the summation of the weights of the covered items. An item j is covered if at least one set containing j is chosen. This is the term $\sum_{j \in T_x} W_j$ in Section 5.2.

Hyperparameter fine-tuning. The overall fine-tuning principles are the same as in the experiments on the facility location problem. See Appendix G.1.2.

Our hyperparameter search space is as follows:

- For UCom2: LR $\in \{1e-1, 1e-2, 1e-3, 1e-4, 1e-5\}$ and CC $\in \{10, 100, 500\}$

²⁴<https://plato.asu.edu/ftp/lptestset/rail>.

- For CardNN: $LR \in \{1e-1, 1e-2, 1e-3, 1e-4, 1e-5\}$ and $\sigma \in \{0.01, 0.15, 0.25\}$

The best hyperparameter settings for each dataset are:

- Rand500:
 - UCom2: $LR = 1e-5$, $CC = 500$
 - CardNN: $LR = 1e-5$, $\sigma = 0.15$
- Rand1000:
 - UCom2: $LR = 1e-5$, $CC = 500$
 - CardNN: $LR = 1e-5$, $\sigma = 0.15$
- Twitch:
 - UCom2: $LR = 1e-1$, $CC = 10$
 - CardNN: $LR = 1e-4$, $\sigma = 0.01$
- Railway:
 - UCom2: $LR = 1e-5$, $CC = 10$
 - CardNN: $LR = 1e-5$, $\sigma = 0.15$

G.1.4. ROBUST COLORING

Here, we provide more details about the settings of the experiments on the robust coloring problem.

Datasets. We use four real-world uncertain graphs (Hu et al., 2017; Ceccarello et al., 2017; Chen et al., 2019). They are available online.²⁵ Some basic statistics of the datasets are as follows:

- **Collins:** $n = 1004$ nodes and $m = 8323$ edges; a deterministic greedy coloring algorithm uses 18 colors for the hard conflicts, and 36 colors for all the conflicts.
- **Gavin:** $n = 1727$ nodes and $m = 7534$ edges; a deterministic greedy coloring algorithm uses 7 colors for the hard conflicts, and 16 for all the conflicts.
- **Krogan:** $n = 2559$ nodes $m = 7031$ edges; a deterministic greedy coloring algorithm uses 8 colors for the hard conflicts, and 25 for all the conflicts.
- **PPI:** $n = 1912$ nodes $m = 22749$ edges; a deterministic greedy coloring algorithm uses 47 colors for the hard conflicts, and 53 for all the conflicts.

We take the largest connected component of each dataset. For each dataset, the 20% edges with the highest edge weights are chosen as the hard conflicts.

Methods. We consider four baseline methods:

- **Greedy-RD:** The method first samples a random permutation of nodes, and then following the permutation, for each node, greedily chooses the best coloring to (1) avoid all the hard conflicts and (2) optimizes the objective; 300 seconds are given on each test graph.
- **Greedy-GA:** This is the method proposed by Yanez & Ramirez (2003) in the original paper of robust coloring. The difference between greedy-RD and greedy-GA is that greedy-GA uses a genetic algorithm (GA) to learn a good permutation instead of randomly sampling permutations; in the GA algorithm, the number of iterations is 20, the population size is 20, the crossover probability is 0.6, the mutation probability is 0.1, the elite ratio is 0.01, the parents proportion is 0.3.

²⁵<https://github.com/Cecca/ugraph/tree/master/Reproducibility/Data>; <https://github.com/stas10217/UKGE/tree/master/data>

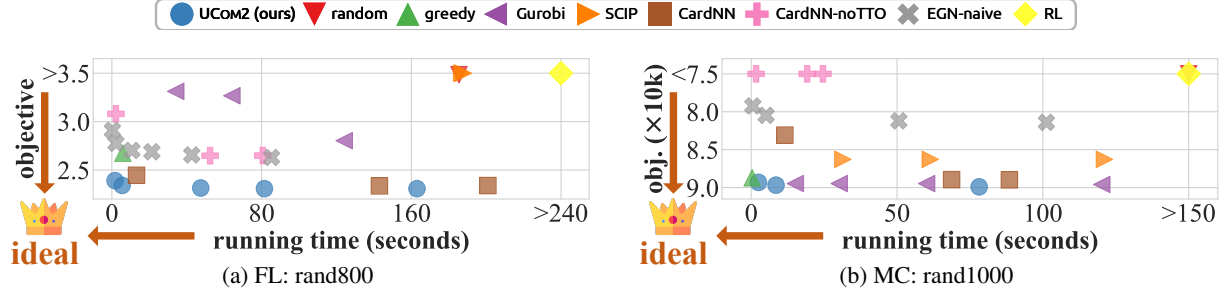


Figure 2: The speed-quality trade-offs on facility location (FL) and maximum coverage (MC). Running time (x -axis): smaller the better. Objective (y -axis): for FL smaller the better; for MC larger the better. For MC, we reverse the y -axis so that the ideal point is always at the bottom left corner. These are results complementing Figure 1.

- **Deterministic coloring (DC):** a deterministic greedy coloring algorithm (Kosowski & Manuszewski, 2004) is used to satisfy all the hard conflicts, and the soft conflicts are included in different random orders until no more soft conflicts can be satisfied. The maximum possible number of soft conflicts that can be included is found by binary search; 300 seconds are given on each test graph.
- **Gurobi:** the problem is formulated as an MIP and the solver is used; 300 seconds are given on each test graph.

Hyperparameters. For UCOM2, we do not fine-tune hyperparameters. We consistently use learning rate $\eta = 0.1$ and the constraint coefficient β is set as the highest penalty on soft conflicts, i.e., $\max_{e=(u,v) \in E_s} \log(1 - P(e))$.

Speed-quality trade-offs. We record the running time of our method using only CPUs and using GPUs. For our method, we start from multiple random initial probabilities (each entry is sampled uniformly at random in $[0, 1]$), while making sure that even with only CPUs, our method uses less time than each baseline.

Evaluation. The recorded objective is the negative log-likelihood of no soft conflicts being violated, i.e., the function f_2 in Section 5.3.

G.2. Full Results

Here, we provide the full raw results on each problem, together with the standard deviations of the results obtained by five random independent trials.

In Figure 2, we provide the trade-off plots for the other datasets, as complementary results to Figure 1.

In Table 4, we provide the full raw results with standard deviations on the facility location problem.

In Table 5, we provide the full raw results with standard deviations on the maximum coverage problem.

G.3. Ablation Studies

Here, we provide the results of ablation studies.

G.3.1. Q1: ARE GOOD PROBABILISTIC OBJECTIVES HELPFUL?

Here, we check whether the probabilistic objectives derived by us are helpful. We compare (a) EGN-naive (non-good objectives and iterative rounding) and (b) UCOM2-iterative (good objectives and iterative rounding). It is difficult to compare the full-fledged version of UCOM2 (good objectives and greedy derandomization) and a variant with non-good objectives and greedy derandomization, because we find computing the incremental differences of non-good objectives nontrivial (yet less meaningful).

In Tables 6 and 7, we show the performance of EGN-naive and UCOM2-iterative on facility location and maximum coverage. We observe that in most cases, the optimization objective with the good objectives is better. However, we also observe that using the good objectives, the running time is sometimes higher. This is because the good objective of cardinality constraints proposed by us is mathematically more complicated than the one used in EGN-naive formulated by Wang et al. (2023), which is $\max(\sum_v p_v - k, 0)$ for the cardinality constraint that at most k nodes are chosen. See also Appendix B.3. This also

Table 4: Full raw results on facility location with the standard deviations. Running time (time): smaller the better. Objective (obj): smaller the better.

method	rand500		rand800		starbucks		mcd		subway	
	obj↓	time↓	obj↓	time↓	obj↓	time↓	obj↓	time↓	obj↓	time↓
random	3.43	240.00	3.48	240.00	0.54	240.00	1.54	240.00	2.72	240.00
(std)	0.006	0.000	0.011	0.000	0.014	0.000	0.029	0.000	0.025	0.000
greedy	2.85	2.10	2.67	5.88	0.35	6.51	1.12	11.51	1.99	26.00
(std)	0.000	0.012	0.000	0.025	0.000	0.032	0.000	0.054	0.000	0.115
Gurobi	2.56	121.86	2.92	125.04	0.31	102.48	1.42	125.20	4.71	138.85
(std)	0.009	0.028	0.019	0.197	0.013	2.328	0.110	0.044	0.633	0.248
SCIP	4.16	94.39	5.43	191.64	5.73	80.51	51.79	485.91	98.47	736.60
(std)	0.012	0.289	0.000	1.234	2.722	2.511	0.000	2.755	0.000	15.188
CardNN-S	2.74	13.94	2.46	16.13	0.47	19.23	1.09	23.50	1.93	20.38
(std)	0.006	0.320	0.003	0.758	0.020	4.722	0.008	1.979	0.015	0.580
CardNN-GS	2.41	71.45	2.34	141.76	0.31	39.88	1.08	42.34	1.85	30.12
(std)	0.002	0.906	0.002	0.713	0.004	1.153	0.014	4.045	0.018	0.788
CardNN-HGS	2.41	100.40	2.34	181.66	0.31	90.93	1.08	96.44	1.83	57.25
(std)	0.001	1.474	0.001	0.849	0.005	4.547	0.024	4.519	0.015	3.947
CardNN-noTTO-S	3.44	2.03	3.57	2.01	0.97	2.03	3.67	1.96	6.33	2.01
(std)	0.067	0.020	0.041	0.032	0.168	0.217	0.227	0.254	0.310	0.016
CardNN-noTTO-GS	2.74	28.61	2.66	51.92	0.44	8.18	1.18	15.73	2.20	4.45
(std)	0.009	0.332	0.008	1.038	0.018	0.093	0.035	1.171	0.077	0.381
CardNN-noTTO-HGS	2.74	37.35	2.65	61.69	0.42	15.59	1.19	28.31	2.17	7.37
(std)	0.012	2.305	0.009	0.350	0.010	0.042	0.024	0.363	0.069	0.039
EGN-naive	2.65	78.80	2.63	85.30	0.33	120.87	1.56	48.08	2.63	120.87
(std)	0.254	9.846	0.134	0.139	0.020	8.679	0.128	8.655	0.777	1.182
RL-transductive	5.57	300.00	5.18	300.00	2.97	1800.00	2.60	1800.00	4.50	1800.00
(std)	0.356	0.000	0.362	0.000	0.245	0.000	0.261	0.000	0.415	0.000
RL-inductive	4.07	300.06	4.27	300.54	0.79	300.04	2.40	300.04	4.23	300.05
(std)	0.227	0.019	0.143	0.157	0.148	0.014	0.241	0.016	0.395	0.015
UCOM2-short	2.51	0.91	2.38	1.91	0.30	0.52	0.99	2.56	1.86	3.56
(std)	0.076	0.084	0.005	0.034	0.003	0.365	0.020	0.154	0.063	1.600
UCOM2-middle	2.41	29.68	2.31	29.90	0.30	2.26	0.95	8.77	1.80	26.23
(std)	0.065	1.755	0.002	1.388	0.004	1.371	0.009	0.207	0.068	3.913
UCOM2-long	2.40	73.86	2.31	59.43	0.29	10.54	0.94	38.04	1.79	45.99
(std)	0.065	4.383	0.002	3.894	0.005	6.114	0.004	0.985	0.078	6.808

validates the necessity of our fast incremental derandomization scheme, which can improve the speed.

G.3.2. Q2: IS GREEDY DERANDOMIZATION BETTER THAN ITERATIVE ROUNDING?

Here, we check whether the proposed greedy derandomization is helpful, especially when compared to the iterative rounding proposed by Wang et al. (2022). We compare (a) the full-fledged version of UCOM2 (good objectives and greedy derandomization) and (b) UCOM2-iterative (good objectives and iterative rounding). In Tables 8 and 9, we show the performance of UCOM2 and UCOM2-iterative on facility location and maximum coverage.

We observe that when using (incremental) greedy derandomization (compared to iterative rounding), UCOM2 archives better optimization objectives within a shorter time, validating that the greedy derandomization scheme proposed by us is indeed helpful.

In conclusion, each component in UCOM2 is helpful in most cases, but only when combining both good objectives with greedy derandomization can we obtain the best synergy.

G.3.3. Q3: DOES INCREMENTAL DERANDOMIZATION IMPROVE THE SPEED?

Here, we want to check how much the proposed incremental derandomization scheme using incremental differences helps in improving the speed. With greedy derandomization, we compare the running time of incremental derandomization and naive derandomization (i.e., evaluating the objective on each possible local derandomization case), on facility location and maximum coverage.

In Tables 10 and 11, we show the running time of UCOM2 when using incremental derandomization and when using naive derandomization, on facility location and maximum coverage.

Table 5: Full raw results on maximum coverage with the standard deviations. Running time (time): smaller the better. Objective (obj): larger the better.

method	rand500		rand1000		twitch		railway	
	obj↑	time↓	obj↑	time↓	obj↑	time↓	obj↑	time↓
random	36874.94	240.00	70756.03	240.00	17756.52	240.00	7333.90	240.00
(std)	22.534	0.000	24.965	0.000	213.655	0.000	3.774	0.000
greedy	44312.81	0.09	88698.89	0.33	33822.40	0.69	7603.00	0.76
(std)	0.000	0.005	0.000	0.006	0.000	0.012	0.000	0.015
Gurobi	44880.59	120.05	89636.32	120.10	33840.40	0.65	7586.40	120.74
(std)	7.132	0.001	22.677	0.004	0.000	0.012	3.878	0.017
SCIP	43805.35	120.07	86274.66	119.49	33840.40	3.28	7585.50	121.48
(std)	4.420	0.002	0.000	0.052	0.000	0.004	0.000	0.025
CardNN-S	42037.90	11.73	83434.44	11.86	33836.16	7.96	7397.10	2.82
(std)	75.443	0.465	143.252	0.808	1.541	0.253	8.834	0.369
CardNN-GS	44737.28	40.33	89313.37	55.95	33840.08	16.50	7616.70	17.64
(std)	7.150	0.430	42.942	0.070	0.640	0.495	4.411	1.221
CardNN-HGS	44742.53	55.64	89330.76	81.95	33840.32	30.73	7619.90	27.25
(std)	5.967	0.972	36.536	0.142	0.160	1.513	4.923	4.501
CardNN-noTTO-S	31283.61	1.83	62120.08	2.04	246.12	0.93	7148.10	1.17
(std)	3431.866	0.149	6841.483	0.334	322.740	0.081	0.490	0.020
CardNN-noTTO-GS	37010.18	10.40	71171.64	20.19	844.52	1.93	7324.40	5.72
(std)	171.453	0.915	464.520	0.293	722.439	0.134	5.571	0.413
CardNN-noTTO-HGS	37012.94	11.93	71198.82	24.80	6594.08	2.35	7324.70	9.23
(std)	173.545	0.635	437.536	0.348	4753.903	0.056	6.508	0.723
EGN-naive	41259.13	120.11	81689.73	120.27	4425.52	120.39	7376.60	120.94
(std)	187.784	0.005	325.560	0.032	5480.695	0.435	7.303	0.420
RL-transductive	41461.65	300.00	73597.20	300.00	32143.20	1800.00	7307.00	1800.00
(std)	580.240	0.000	957.157	0.000	315.444	0.000	53.139	0.000
RL-inductive	34536.00	300.06	69155.00	300.18	19840.60	301.91	7320.50	301.78
(std)	22.154	0.017	42.216	0.022	55.146	0.254	9.578	0.195
ours-short	44622.79	0.96	89130.65	1.83	33828.40	1.82	7607.10	2.00
(std)	9.158	0.106	33.987	0.116	0.000	0.145	4.329	0.055
ours-middle	44971.97	15.16	89496.45	7.84	33828.40	11.43	7617.80	16.05
(std)	16.313	1.057	29.199	0.117	0.000	0.301	4.007	0.135
ours-long	45000.41	30.02	89721.94	73.54	33828.40	19.35	7620.50	16.09
(std)	16.399	2.097	23.553	1.007	0.000	0.578	5.206	0.118

Table 6: Ablation study on facility location: are good probabilistic objectives helpful? Running time (time): smaller the better. Objective (obj): smaller the better.

method	rand500		rand800		starbucks		mcd		subway	
	obj↓	time↓	obj↓	time↓	obj↓	time↓	obj↓	time↓	obj↓	time↓
EGN-naive	2.65	78.80	2.63	85.30	0.33	120.87	1.56	48.08	2.63	120.87
UCOM2-iterative	2.65	169.56	2.67	205.12	0.33	162.15	1.05	87.45	1.96	52.37

Table 7: Ablation study on maximum coverage: are good probabilistic objectives helpful? Running time (time): smaller the better. Objective (obj): larger the better.

method	rand500		rand1000		twitch		railway	
	obj↑	time↓	obj↑	time↓	obj↑	time↓	obj↑	time↓
EGN-naive	41378.43	120.72	81393.77	101.23	15448.20	120.72	7290.00	120.76
UCOM2-iterative	42820.04	131.78	84397.79	209.95	16093.80	137.08	7304.50	120.21

Table 8: Ablation study on facility location: is greedy derandomization better than iterative rounding? Running time (time): smaller the better. Objective (obj): smaller the better.

method	rand500		rand800		starbucks		mcd		subway	
	obj↓	time↓	obj↓	time↓	obj↓	time↓	obj↓	time↓	obj↓	time↓
UCOM2-iterative	2.65	169.56	2.67	205.12	0.33	162.15	1.05	87.45	1.96	52.37
UCOM2-short	2.51	0.91	2.38	1.91	0.30	0.52	0.99	2.56	1.86	10.35
UCOM2-middle	2.41	29.68	2.31	29.90	0.30	2.26	0.95	8.77	1.80	26.23
UCOM2-long	2.40	73.86	2.31	59.43	0.29	10.54	0.94	38.04	1.79	45.99

Table 9: Ablation study on maximum coverage: is greedy derandomization better than iterative rounding? Running time (time): smaller the better. Objective (obj): larger the better.

method	rand500		rand1000		twitch		railway	
	obj↑	time↓	obj↑	time↓	obj↑	time↓	obj↑	time↓
UCOM2-iterative	42820.04	131.78	84397.79	209.95	16093.80	137.08	7304.50	120.21
UCOM2-short	44622.80	0.96	89130.70	1.83	33828.40	1.82	7607.10	2.00
UCOM2-middle	44972.00	15.16	89496.50	7.84	33828.40	11.43	7616.00	8.17
UCOM2-long	45000.40	30.02	89721.90	73.54	33828.40	19.35	7620.50	16.04

Table 10: Ablation study on facility location: does incremental derandomization improve the speed?

	rand500	rand800	starbucks	mcd	subway
naive derandomization	317.46	1061.02	231.85	1710.84	10196.05
incremental derandomization	0.37	1.70	1.28	3.56	11.25
speed-up ratio	849.65	623.30	180.77	480.14	906.30

Table 11: Ablation study on maximum coverage: does incremental derandomization improve the speed?

	rand500	rand1000	twitch	railway
naive derandomization	240.77	1186.06	2247.88	359.86
incremental derandomization	0.91	2.48	1.82	1.90
speed-up ratio	265.49	478.14	1231.81	189.52

We observe that using incremental derandomization significantly improves the derandomization speed, and the superiority is usually more significant when the dataset sizes increase.

G.3.4. Q4: HOW DOES UCOM2 PERFORM WITH DIFFERENT CONSTRAINT COEFFICIENTS?

Here, we want to check how UCOM2 performs when using different constraint coefficients (i.e., different β values) and fixing the other hyperparameters.

In Tables 12 to 14, we show the performance of UCOM2 when using different β values, on facility location, maximum coverage, and robust coloring.

For facility location and maximum coverage, the candidate β values are the same as in Appendices G.1.2 and G.1.3. We use the fastest version of UCOM2 without test-time augmentation.

For robust coloring, let the originally used $\beta_0 := \max_{e \in E_s} \log(1 - P(e))$, we consider three candidate values: $\frac{1}{2}\beta_0$, β_0 , and $2\beta_0$. The other hyperparameters are fixed as the same.

Our observations are as follows. For facility location and maximum coverage:

- For random graphs, since the distribution of the training set and the distribution of the test set are the same, the originally used β values perform well, usually the best among the candidates.
- For real-world graphs, the originally used β values do not achieve the best performance in some cases. In our understanding, this is because we use the smallest graph in each group of datasets as the validation graph, while the smallest graph possibly has a slightly different data distribution from the other graphs in the group, i.e., the test set.
- Overall, certain sensitivity w.r.t β can be observed, but usually, multiple β values can achieve reasonable performance.

For robust coloring:

- Overall, all the candidates β values can achieve similar performance.
- In other words, the performance of our method is not very sensitive to the value of β on robust coloring.

Table 12: Ablation study on facility location: how does UCOM2 perform with different constraint coefficients? The results with the constraint coefficient originally used in our experiments are marked in bold. The numbers here are objectives (smaller the better).

β	rand500	rand800	starbucks	mcd	subway
1e-1	2.50	2.47	0.31	1.02	1.75
1e-2	2.51	2.38	0.30	0.99	1.86
1e-3	3.19	2.79	1.85	1.41	3.83

Table 13: Ablation study on maximum coverage: how does UCOM2 perform with different constraint coefficients? The results with the constraint coefficient originally used in our experiments are marked in bold. The numbers here are objectives (larger the better).

β	rand500	rand1000	twitch	railway
10	43744.80	87165.08	33801.80	7607.10
100	44382.36	88543.73	33828.40	7602.00
500	44622.80	89130.70	33825.80	7575.50

Table 14: Ablation study on robust coloring: how does UCOM2 perform with different constraint coefficients? The results with the constraint coefficient originally used in our experiments are marked in bold. The numbers here are objectives (smaller the better).

β	collins		gavin		krogan		ppi	
	18 colors	25 colors	8 colors	15 colors	8 colors	15 colors	47 colors	50 colors
$\frac{1}{2}\beta_0$	78.32	15.61	46.56	6.70	52.04	0.87	2.93	1.01
β_0 (originally used)	82.26	15.16	42.99	6.72	52.44	0.87	2.93	1.01
$2\beta_0$	81.17	15.83	44.96	6.77	55.25	0.87	2.93	1.01

H. Discussions

H.1. Inductive Settings and Transductive Settings

As discussed in Appendix B.1, the differentiable optimization in the pipeline can be done either in an inductive setting or in a transductive setting. Although ideally, a well-trained encoder can save much time without degrading the performance, in practice, inductive settings can be less effective (Li et al., 2023), especially when the training set and the test set have very different distributions (Drakulic et al., 2023).

As shown in our experimental results, the performance of CardNN (Wang et al., 2023) highly relies on test-time optimization (compare CardNN and CardNN-noTTO), which implies that the training is actually less essential than the direct optimization on test instances.

For UCOM2, we also observe that, when the training set and the test set are from different distributions, the training can be less helpful. Even applying derandomization on random probabilities can work well sometimes (but not always).

H.2. Reinforcement Learning and Probabilistic-Method-Based UL4CO

The connections between reinforcement learning and probabilistic-method-based UL4CO have been discussed by Wang et al. (2022). The direct connection comes from the fact that the policy gradient tries to approximate expectations by sampling, while probabilistic-method-based UL4CO aims to directly evaluate expectations.

Differences also exist. In many cases, RL methods generate decisions in an autoregressive manner, while UL4CO methods try to do it in a one-shot manner (Wang et al., 2023), although one-shot RL has also been recently considered (Viquerat et al., 2023). Both the overhead of sampling and the autoregressive decision-encoding can potentially explain why UL4CO is usually more efficient than RL methods.

We focus on cases under complex conditions in this work. In RL, there are also similar subfields studying RL under constraints. On top of the basic difficulties of “sampling”, constrained sampling for RL is even trickier and less efficient. Moreover, the analysis has been limited to simple constraints, e.g., linear and convex ones (Miryoosefi & Jin, 2022). We believe that this work shows that UL4CO is especially promising in cases under complex conditions.